Mon. Not. R. Astron. Soc. **381,** 401–417 (2007) doi:10.1111/j.1365-2966.2007.12299.x

Properties of bars and bulges in the Hubble sequence

E. Laurikainen,[1]⋆ H. Salo,[1] R. Buta[2] and J. H. Knapen[3,4]

[1]*Division of Astronomy, Department of Physical Sciences, University of Oulu, Oulu FIN-90014, Finland*
[2]*Department of Physics and Astronomy, University of Alabama, Box 870324, Tuscaloosa, AL 35487, USA*
[3]*Instituto de Astrofísica de Canarias, E-38200 La Laguna, Spain*
[4]*University of Hertfordshire, Centre for Astrophysics Research, Hatfeld, Herts AL10 9AB*

Accepted 2007 July 30. Received 2007 June 8; in original form 2007 February 19

ABSTRACT

Properties of bars and bulges in the Hubble sequence are discussed, based on an analysis of 216 disc galaxies of S0-Sm types (S0s from the Near-Infrared S0 Survey and spirals from the Ohio State University Bright Spiral Galaxy Survey). For this purpose we have collected, and completed when necessary, the various analyses we have previously made separately for early- and late-type galaxies. We find strong evidence of pseudo-bulges in all Hubble types. Pseudo-bulges are disc-like structures formed by secular evolutionary processes in galaxies. Similar to spirals, the early-type disc galaxies (S0-S0/a) have on average relatively exponential bulges with Sersic index $n < 2$, and 56 per cent of them show disc-like fine structures in the region of the bulge. For some of the galaxies there is also kinematic evidence of pseudo-bulges. If S0-S0/a galaxies were once spirals, stripped of their gas, then redistributed gas and star formation in the disc would be a natural explanation for all pseudo-bulges in the Hubble sequence. However, it is difficult to explain how the bulges of S0 galaxies, which typically include about 30 per cent of the total galaxy mass, were formed by secularly induced central star formation. A more likely explanation is that pseudo-bulges in barred early-type galaxies are a combination of secularly induced star formation and the central steepening of the old stellar distribution. Bulges in non-barred early-type galaxies could be either classical merger-built bulges, or pseudo-bulges formed by similar processes as in barred galaxies, but in response to massive ovals or lenses (70 per cent of S0-S0/a galaxies have ovals/lenses). Observational support for the outlined picture comes from the fact that bars in early-type galaxies seem more evolved: their bars are long and massive and frequently (40 per cent) have ansae morphologies. In this scenario it would be possible also to explain why barred early-type galaxies (preferentially pseudobulges) have slightly smaller B/T flux ratios than the non-barred early-type galaxies (mostly classical bulges).

Key words: galaxies: elliptical and lenticular, cD – galaxies: evolution – galaxies: structure.

1 INTRODUCTION

One central goal of extragalactic research is to understand what factors drive the morphology of galaxies and how important these factors are over long-term evolution. In the present view the early Universe was dominated by hierarchical clustering and galaxies were formed from the density fluctuations of cold dark matter (Searle & Zinn 1978; White & Rees 1978; Steinmetz & Navarro 2002). The processes were rapid and violent, leading to massive starbursts in merging systems and finally to the formation of elliptical galaxies and the spheroidal components of disc galaxies. As the Universe expands galaxy mergers become less common and the evolution is governed more by slow secular processes, related to interactions involving collective phenomena, such as bars, ovals or the dark matter haloes in galaxies (see Kormendy & Kennicutt 2004; hereafter KK2004). An important question is how important these secular processes are for the overall evolution of galaxies, and in which way these processes are driven in galaxies.

The hierarchical clustering model seems to account remarkably well for the large-scale structure of galaxies, but has difficulties explaining some structural components of individual galaxies, like lack of cuspy haloes (Bosma 2003) or the number of baryons locked up in dynamically hot spheroidal components (Schechter & Dressler 1987; Fukugita, Hogan & Peebles 1998). Indeed, the origin of bulges is one of the key issues in our understanding of galaxy evolution: are they mainly merger-built classical bulges, or more likely pseudo-bulges formed out of disc material? As discussed by KK2004 and

⋆E-mail: eija.laurikainen@oulu.fi

Athanassoula (2005), pseudo-bulges can have several distinct formation mechanisms, but the main issue such bulges have in common is that they keep a record of their discy origin. Although not straightforward, it is this discy origin that makes it possible to observationally distinguish pseudo-bulges from classical bulges (see Section 3 for details).

There is both observational and theoretical evidence that pseudo-bulges are most efficiently formed in low-luminosity galaxies. Bulges in intermediate-type spirals are predominantly found to be pseudo-bulges (Andredakis, Peletier & Balcells 1995; Carollo, Stiavelli & Mack 1998), and in particular all late-type spirals, which are dominated by low-luminosity galaxies, have pseudo-bulges. These observations are consistent with the so-called 'downsizing effect' (Cowie, Songaila & Hu 1996) within the hierarchical clustering paradigm. Accordingly, the most massive galaxies were formed in the early phases of the Universe, having only modest star formation in the disc after the principal starburst event, whereas dimmer galaxies, in which most of the gas was not washed out in the main starburst event, continue actively forming stars until redshift zero (Cowie et al. 1996; Steffen et al. 2003; Ueda et al. 2003). Although this makes it possible to understand the appearance of pseudo-bulges in low-luminosity spirals, it is noteworthy that many luminous galaxies also have pseudo-bulges. In fact, there is recent evidence showing that this is the case also for many luminous S0 galaxies (Laurikainen, Salo & Buta 2005; Laurikainen et al. 2006a).

In principle, the appearance of pseudo-bulges in S0 galaxies can be understood if S0s are former spirals, stripped out of gas. However, unless significant external gas accretion is assumed, normal spiral galaxies do not have sufficient gas to form the masses of the bulges typically found in early-type galaxies. Such an estimate was made by KK2004, based on the observed gas content and star formation rate for an unbiased sample of 44 nearby galaxies. They estimated that gas accretion episodes will form pseudo-bulges within the mass range of 10^7– $10^{10}\,M_0$. This implies that only bulges in Sc-type spirals could be formed by star formation in the disc. Galaxy evolution in the Hubble sequence can change the morphological type, but it is not expected to be more than one Hubble-type index bin. Even if the bulge-to-total (B/T) mass ratios were considerably smaller (see Laurikainen et al. 2005), it would still be difficult to make the bulges of typical S0 galaxies by star formation in the disc. It is important to re-investigate how the properties of bulges in galaxies of different Hubble types compare with each other, and how the formation histories of the bulges can be understood.

In this study the properties of bars, bulges and ovals in the Hubble sequence are studied and compared with various dynamical models in the literature. In order to characterize the nature of bulges we use a photometric approach by applying a 2D multicomponent decomposition method (Laurikainen et al. 2005), and for a subsample of galaxies stellar kinematic observations are also collected from the literature. The properties of bars and ovals in the same galaxies are derived by Fourier techniques. The decompositions and most of the Fourier analysis for the individual galaxies have been published in a series of papers by us (Buta et al. 2004; Laurikainen et al. 2004b,a; Buta et al. 2005; Laurikainen et al. 2005; Buta et al. 2006; Laurikainen et al. 2006a). Our aim in this paper is to combine all the analysis of the early- and late-type galaxies, and bring them together for a more general discussion in the Hubble sequence. Also, if any of the discussed parameters were not derived earlier for the whole sample of 216 galaxies, the analysis is completed in this study. Such parameters are the ellipticities and the lengths of the bars for the early-type galaxies, and the Fourier amplitude profiles and bar morphologies for the late-type galaxies. Some preliminary results of this study have been reported in the IAUS 235 conference proceeding by Laurikainen, Salo & Buta (2006b).

2 SAMPLE

The sample used in this study consists of 216 galaxies, based on the Ohio State University Bright Spiral Galaxy Survey (OSUBSGS; Eskridge et al. 2002) for spirals, and on the Near-Infrared S0 Galaxy Survey (NIRS0S; Laurikainen et al. 2005; Buta et al. 2006) for S0-S0/a galaxies. Both are magnitude-limited samples ($B_{\rm T} < 12.5$) avoiding high-inclination galaxies (INC $< 65°$). The NIRS0S sample has been observed only partly so far, but when combined with the OSUBSGS, a reasonably sized sample is obtained to study the properties of bars and bulges in the Hubble sequence. Fig. 1 (middle panel) shows the mean absolute galaxy magnitudes in the $K_{\rm s}$ band in each Hubble-type index bin. The magnitudes are integrated $K_{\rm s}$-band magnitudes to the limiting surface brightness of 20 mag arcsec^{-2}, corrected for Galactic extinction. The magnitudes are from the Two Micron All Sky Survey (2MASS)[1] and the extinction values are from the NASA/IPAC Extragalactic Database (NED).[2] The mean absolute magnitudes of the galaxies in our sample are very similar for the different Hubble types, except for galaxies of types Sc and later classes, which are dominated by dwarf galaxies. A large majority of the galaxies in our sample are luminous: they are slightly brighter than the characteristic absolute magnitude $M_{K_{\rm s}} = -23.1$ in Schechter's luminosity function (Gardner et al. 1997). The analysis discussed in this paper is based primarily on H-band (for OSUBSGS sample) and $K_{\rm s}$-band (for NIRS0S sample) images.

3 THE CONCEPT OF A PSEUDO-BULGE

The early observational assessments of bulges were based on the ellipticity of the isophotes in the inner and outer discs (Kent 1986; Andredakis et al. 1995). Alternatively, bulges were identified as extra light above the exponential disc in the central parts of the galaxies (Carollo et al. 1999). A more physical approach was achieved by dividing the bulges into classical and pseudo-bulges. Classical bulges are assumed to be formed by dissipative gas processes before the present discs were formed, whereas pseudo-bulges were formed later by gas and stellar dynamical processes in the galactic discs. The idea that pseudo-bulges form by slow secular processes after the initial rapid phase of galaxy formation was first suggested by Kormendy in 1982.

The procedure for identifying a pseudo-bulge can be mainly observational (see the recent review by KK2004), or based on N-body simulations, related to the formation histories of pseudo-bulges (see Athanassoula 2005). Both approaches have their advantages, but it seems that both studies have led to a fairly similar understanding of pseudo-bulges: they are considered to be either products of star formation in the central regions of the discs, or products related to the evolution of the orbital families of bars. In the following we list the main observational criteria to identify pseudo-bulges, as given by

[1] The 2MASS, which is a joint project of the University of Massachusetts and the Infrared Processing and Analysis Center/California Institute of Technology, is funded by the National Aeronautics and Space Administration and the National Science Foundation.

[2] The NED is operated by the Jet Propulsion Laboratory, California Institute of Technology, under contract with the National Aeronautics and Space Administration.

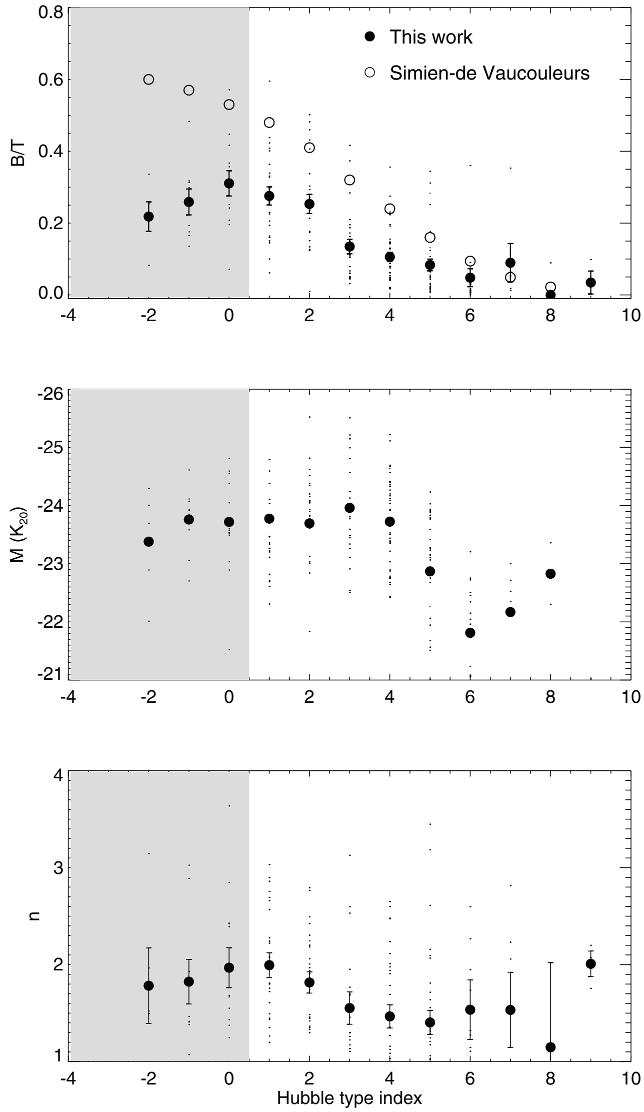

Figure 1. The *B*/*T* flux ratio (upper panel), the absolute *H*-band galaxy luminosity using the magnitudes to the surface brightness of 20 mag arcsec^{-2} taken from the NED and corrected for Galactic extinction (middle panel), and the shape parameter of the bulge, *n* corresponding to Sersic function (lower panel), as a function of the Hubble-type index. These parameters are calculated for our sample of 216 galaxies. The large symbols indicate mean values and the error bars are standard deviations of the mean. For comparison, in the upper panel the measurements by Simien & de Vaucouleurs (1986), obtained in the *B* band (1986) are also shown. Our parameters of the bulges are derived from K_s and *H*-band images.

KK2004. An apparent bulge is a pseudo-bulge if it satisfies several or even all of the following criteria.

(1) It has spiral structure or a flattening similar to that of the outer disc.
(2) It contains a nuclear bar.
(3) It is box shaped.
(4) It has Sersic index $n = 1$– 2.
(5) It is more rotation dominated than are classical bulges.
(6) It is a lower velocity dispersion outlier in the Faber & Jackson (1976) correlation between apparent bulge luminosity and velocity dispersion.
(7) It is dominated by Population I material (young stars, gas, dust), but there is no sign of a merger process.

KK2004 also suggested that if the *B*/*T* luminosity ratio is less than 0.5, it seems fairly safe to conclude that the galaxy contains a pseudo-bulge. Based on the theoretical approach by Athanassoula (2005), we extend point 3 in the following manner.

(3′) A bulge is a pseudo-bulge if it has a box/peanut shaped structure (in inclined galaxies) nearly aligned with the main part of the bar and is clearly shorter than the bar.

These are also the criteria we follow to identify pseudo-bulges in this study. We do not yet have the stellar population indices or all the kinematic observations available, but for identifying pseudo-bulges in a reliable manner it is enough to fulfil only some of the above criteria. According to theoretical models (Athanassoula & Misioritis 2002, their fig. 5; see also Athanassoula 2005) a pseudo-bulge can also be a centrally concentrated, nearly exponential part of the bar inside a vertically thickened structure. However, the photometric properties of this kind of pseudo-bulge are similar to other disc-like bulges. In simulations the vertically thickened boxy/peanut structures are generally studied only in galaxies with nearly edge-on inclinations.

4 OBSERVATIONAL EVIDENCE OF PSEUDO-BULGES IN THE HUBBLE SEQUENCE

4.1 Photometric approach

In the following we use a 2D multicomponent decomposition algorithm (Laurikainen et al. 2005) to derive the *B*/*T* flux ratios and the Sersic parameters of the bulges. The method takes into account not only the bulges and discs, but also multiple bars, ovals or central discs. For the bulges a generalized Sersic $r^{1/n}$ function is used, whereas bars and ovals are typically fitted with a Ferrers function. Because ovals and lenses typically have more uniform surface brightness distributions than bars, fairly flat Ferrers functions with $n = 1$ are generally used for fitting them. In some cases a Sersic function gives the best fit for the central disc. Subtracting the bulge model or the disc model from the original image is then a sensitive way for identifying the inner morphological structures of these galaxies. In some cases unsharp masks were also used. The decompositions for the individual galaxies discussed in this paper have been presented previously by Laurikainen et al. (2004b, 2005, 2006a) and Laurikainen et al. (2004a).

4.1.1 Innermost structures of the discs

In extensive studies, Carollo and her collaborators (Carollo et al. 1997, 1998, 2002) have shown that late-type spirals (Sb-Sbc) frequently have star-forming nuclear rings, inner spiral arms and inner discs. In many cases the inner discs are the only bulge-like structures in these galaxies, and some galaxies have no bulge at all. A pseudo-bulge has been recently found also in one early-type spiral galaxy, NGC 7690, by Kormendy et al. (2006), based on the photometric properties of the bulge. For some spiral galaxies there is also kinematic evidence confirming the disc-like nature of the bulge (Falcön-Barroso et al. 2003; Cappellari et al. 2005). For S0-S0/a galaxies the frequency of inner structures is here derived by combining the data presented by Laurikainen et al. (2005) and Laurikainen et al. (2006a). We confirm the earlier result by Laurikainen et al. (2006a) showing that 56 per cent of S0-S0/a galaxies have nuclear bars, nuclear discs or nuclear rings inside the bulge. This would be difficult to understand if these bulges were hot components supported by random motions of stars.

4.1.2 *B/T flux ratios*

One of the main results of our decomposition studies is the typical *B/T* flux ratio which we find to be considerably smaller than found in the previous studies, particularly for the early-type galaxies. In Fig. 1 (upper panel) this is shown, for the first time, for all Hubble types. For comparison, the mean *B/T* flux ratios derived by Simien & de Vaucouleurs (1986) in the *B* band are also shown. The sample of 98 galaxies used in their study included both barred and non-barred galaxies. The difference to our result is significant: while for S0-S0/a galaxies Simien & de Vaucouleurs (1986) found $\langle B/T\rangle_B = 0.57$, we find $\langle B/T\rangle_K = 0.25 \pm 0.10$. One may ask whether this is a wavelength effect, related to different mass-to-luminosity (*M/L*) ratio, or due to the different decomposition methods used. If this were a wavelength effect we should conclude that recent star formation (visible in the *B* band) in the bulge, relative to that in the disc, should be particularly significant in S0 galaxies, which is highly improbable. That the difference is not a wavelength effect becomes clear also by comparing our result with the decompositions made by de Souza, Gadotti & dos Anjos (2004) in the *K*-band. Using their measurements (their table 1) we find $\langle B/T\rangle_K = 0.64$ for S0s, which is very similar to that obtained by Simien & de Vaucouleurs (1986) in the *B* band. A correction related to different star formation timescales at different wavelengths (taken from Schultz et al. 2003) is fairly small: it would change the $(B/T)_K = 0.64$ to $(B/T)_B = 0.54$ (see Laurikainen et al. 2005, for more details).

So, obviously wavelength does not explain the large difference in *B/T* flux ratio between this study and that by Simien & de Vaucouleurs (1986). A more likely explanation is that the more accurate 2D multicomponent decomposition approach used in our study accounts for the effects of strong bars and ovals, structures which in the 1D (used by Simien & de Vaucouleurs 1986) or 2D two-component bulge/disc decompositions (used by de Souza et al. 2004) are easily degenerated with the bulges. In fact, it was shown by Laurikainen et al. (2006a) that, when applied to barred galaxies, both 1D and 2D bulge/disc decompositions give fairly similar high *B/T* flux ratios, whereas 2D bulge/disc/bar decompositions give significantly lower *B/T* flux ratios. Laurikainen et al. (2005) also used synthetic data to demonstrate that most of the bar flux is erroneously assigned to the bulge if a simple bulge/disc decomposition algorithm is applied to a system with a prominent bar. The $(B/T)_H$ flux ratios we find for spiral galaxies are also smaller than those obtained by Simien & de Vaucouleurs (1986), but the differences are much smaller, presumably because bars in later type galaxies are smaller and therefore affect less the decompositions.

The mean *B/T* flux ratios we find are smaller than those typically found for classical bulges (see KK2004). If we assume that the *M/L* ratio is constant in these galaxies, the derived flux ratios are also approximations of the relative masses of bulges. In that case our result contradicts the earlier understanding according to which bulges and discs represent approximately equal amounts of mass in galaxies (Schechter & Dressler 1987; Benson, Frenk & Sharples 2002). Nevertheless, a constant *M/L* ratio might be valid for the discs, but not necessarily in the central regions of the galaxies. If the bulges are redder than the disc, then higher *M/L* ratios should be used for bulges (Bell & de Jong 2001). The conversion of flux ratios to mass ratios is postponed to a forthcoming paper, where colour index maps of our sample will be studied.

4.1.3 *Sersic parameters of the bulge*

Another important finding in this study is that the Sersic parameter n of the bulge is on average $\leqslant 2$ for all morphological types (Fig. 1, lower panel). In the generalized Sersic function the value $n = 1$ corresponds to an exponential disc and $n = 4$ to the de Vaucouleurs-type surface brightness profile. Our result contradicts the view according to which only galaxies later than type Sb have exponential disc-like bulges (Carollo et al. 1998; see also KK2004).

We next look at how this result compares with those obtained in previous studies. It has been shown both for spiral (Andredakis & Sanders 1994) and elliptical galaxies (Caon, Cappaccioli & D'Onofrio 1993) that for the spheroidal component the generalized Sersic function (used also in this study) gives a better fit than the $r^{1/4}$ law. Using a Sersic function for the bulge both Andredakis et al. (1995) and de Souza et al. (2004) found large n values, particularly for S0 galaxies ($\langle n\rangle = 3.7$ and 4.1, respectively), whereas Graham (2001) found $\langle n\rangle = 2$ for the galaxies with the same morphological types. The n values given by Graham are similar to those obtained by us. How can we understand these disagreeing results? One of the key issues is that the sample by Graham did not include barred galaxies, thus any problems related to the degeneracy of bars and bulges were avoided. Most probably the relative masses of bulges were overestimated in the decompositions by Andrekakis et al., thus leading also for an overestimate of the n values. Balcells et al. (2003) have shown the importance of high image resolution when deriving the n values in decompositions. They showed that decompositions where ground-based images are combined with high-resolution *Hubble Space Telescope* images, give considerably lower n values than the decompositions where only ground-based images are used. Small *B/T* flux ratios and n values for S0-S0/a galaxies have been previously reported by Laurikainen et al. (2005) and Laurikainen et al. (2006a). Small n values for barred S0s have been reported also by Aguerri et al. (2005).

4.1.4 *Correlations between the derived parameters*

We confirm the earlier result by Balcells, Graham & Peletier (2004) that galaxies are not scale free, the scale parameter being the relative mass of the bulge (see Fig. 2): both the Sersic parameter n and the effective radius of the bulge normalized to the scalelength of the disc, $r_{\rm eff}/h_{\rm R}$, correlate with *B/T* flux ratio. A critical *B/T* value seems to be 0.1, below which the bulge profiles are close to pure exponentials having $n \sim 1$, thus confirming the disc-like nature of the bulges in these galaxies.

The *K*-band absolute magnitudes provide an interesting additional piece of information. For the late-type spirals the *B/T* flux ratio increases nearly linearly towards brighter galaxies, whereas for the more early-type systems (S0-Sab) the *B/T* flux ratio is independent of the galaxy brightness (Fig. 2, lower panel). The correlation between *B/T* flux ratio and the galaxy brightness is not straightforward to interpret, because there are several mechanisms that might cause this correlation (see discussion in Section 6).

If bars are important drivers of making pseudo-bulges in galaxies we would expect to see some differences in the *B/T* flux ratio between barred and non-barred galaxies within one Hubble-type index bin. This comparison is shown in Fig. 3. The barred classification is based on the de Vaucouleurs Atlas of Galaxies by Buta, Corwin & Odewahn (2007). If the galaxy did not appear in the Atlas, the classification was taken from The Third Reference Catalogue of Bright Galaxies (de Vaucouleurs et al. 1991; hereafter RC3). The RC3 classifications for S0 galaxies are fairly reliable,

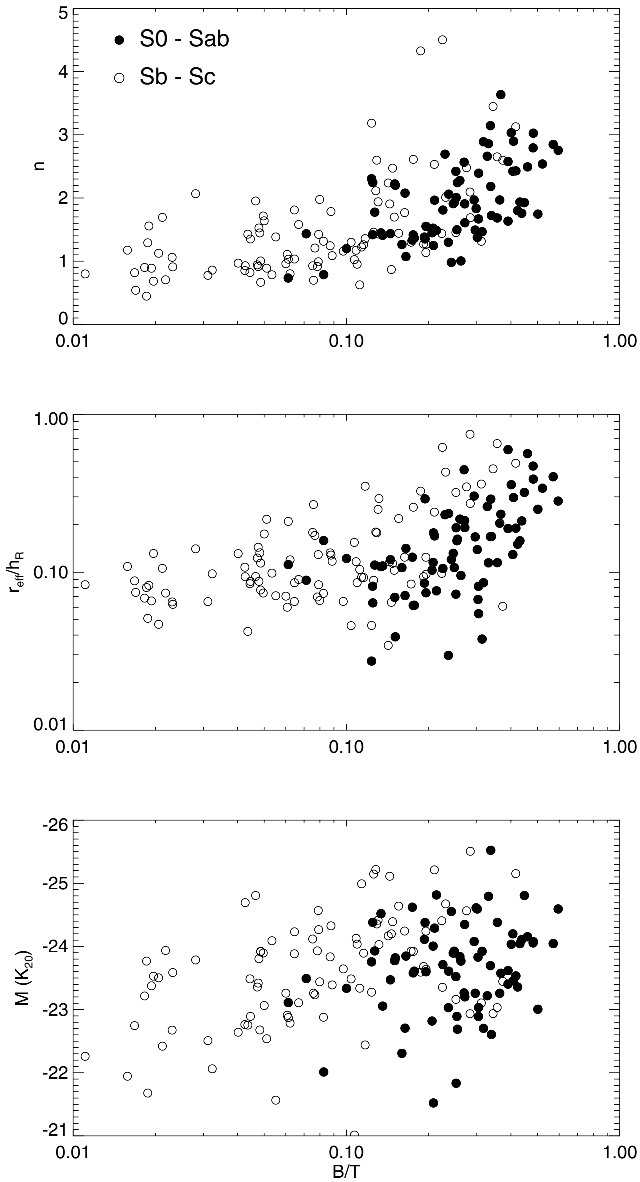

Figure 2. For the same sample are shown the Sersic index of the bulge (upper panel), the effective radius of the bulge, scaled to the scalelength of the disc (middle panel), and the absolute galaxy luminosity (lower panel), as a function of *B*/*T*. The scalelengths are measured from the near-IR images by applying a multicomponent decomposition. The parameters are shown separately for the S0-Sab galaxies, and for the Sb-Sc type spirals.

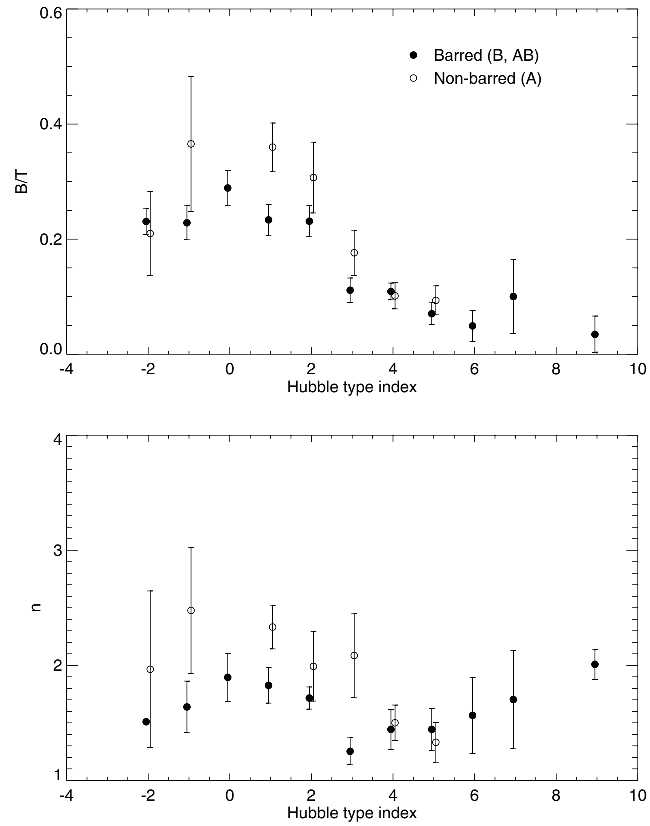

Figure 3. The parameters of the bulge, *B*/*T* and *n*, are shown separately for barred and non-barred galaxies as a function of the Hubble-type index. The classification of barred/non-barred is taken from 'The de Vaucouleurs Atlas of Galaxies' by Buta et al. (2007). Again, the symbols are mean values and the error bars indicate the standard deviations of the mean values.

and independent of the identification method, because S0 galaxies have only a small amount of dust, and the bars do not have a spiral-like nature as in some spiral galaxies. We find that among spiral galaxies later than Sa the properties of bulges are similar for barred and non-barred galaxies, whereas among the earlier type systems the barred galaxies have more exponential bulges. They also have slightly smaller relative bulge masses than the non-barred galaxies. We tested whether the differences are statistically significant. For that purpose the Kolmogorov–Smirnov test was used, grouping together all morphological types with $T \leqslant 2$. According to this test the differences between barred and non-barred galaxies are real: the probability that their *n* parameters are from the same distribution is only 0.02. The same result was found for the *B*/*T* flux ratios. A similar test for later type galaxies ($T > 2$) indicated no difference between barred and non-barred galaxies, as anticipated from Fig. 3.

As any decomposition method, also our multicomponent approach has its limitations. A critical question is whether the uncertainties of the algorithm itself are so large that they alone could produce the differences found between the barred and non-barred galaxies. One way of evaluating this is to look at how much massive nuclear bars can affect the *B*/*T* flux ratio in the decompositions. This evaluation was done by Laurikainen et al. (2005). They showed that although the primary bar can considerably affect both the *B*/*T* flux ratio and the Sersic index *n*, including an additional nuclear bar to the fit does not affect the *n* value at all. It can decrease the mean *B*/*T* flux ratio by 0.05, which is slightly smaller than the difference in *B*/*T* flux ratio between the barred and non-barred galaxies.

4.2 Kinematic approach

The kinematic approach for detecting pseudo-bulges was first suggested by Illingworth (1977): classical bulges are supported by random motions of stars (Illingworth 1981), whereas pseudo-bulges are dominated by rotational velocities (Kormendy 1981). A useful discriminator is the parameter $V_{\max}/\sigma$ versus ϵ (Illingworth 1977; Kormendy 1982), where $V_{\max}$ is the maximum rotational line-of-sight velocity of the bulge measured from the absorption lines, σ is the mean stellar line-of-sight velocity dispersion of the bulge just outside the nucleus, and ϵ is the characteristic ellipticity inside the

Table 1. Stellar kinematical properties of bulges. The columns are explained in the text.

Galaxy	T	INC/PA (°)	$V_{\max}$ (km s^{-1})	σ (km s^{-1})	ϵ	r (arcsec)	Reference
NGC 210	3	49.2/162.7	83.3	120	0.1	10	Pizzella et al. (2004)
NGC 936	−1	42.4/123	80.2	175	0.15	5	Kormendy (1983)
NGC 1400	−3	23.8/37	90.0	266	0.1	5	Bertin et al. (1994)
NGC 1553	−2	41.5/150	99.4	162	0.4	10	Kormendy (1984)
NGC 1574	−3	16/31	39.9	180	0.1	6	Jarvis et al. (1988)
NGC 2681	0	24.2/102	20.1	111	0.2	5	McElroy (2004), Moiseev, Valdës & Chavushyan (2004)
NGC 2775	2	36.8/166.5	125.2	175	0.11	<20	Corsini et al. (1999)
			100.0	140	0.11	<20	Shapiro, Gerssen & van der Marel (2003)
NGC 2855	0	33.1/107	120.0	190	0.17	10	Corsini, Pizzella & Bertola (2002)
NGC 2983	−1	54.8/91	54.7	160	0.2	2	Bettoni, Galletta & Vallenari (1988)
NGC 3169	1	39.1/58.0	112.0	171	0.36	10	Heraudeau & Simien (1998)
NGC 3626	−1	48.0/159	150.0	142	0.4	5	Haynes et al. (2000)
NGC 3706	−4	50.65/76	139.9	281	0.38	10	Carollo, Danziger & Buson (1993) and Carollo & Danziger (1994)
NGC 3810	5	47.2/23.1	50.0	73	0.27	15	Heraudeau et al. (1999)
NGC 3941	−2	49.4/7	60.0	131/150	0.2	5	Fisher (1997), Denicolö et al. (2005)
NGC 4138	1	53.3/148.2	100.0	161	0.21	5	Jore, Broeils & Haynes (1996)
NGC 4340	−1	56.2/99	48.2	115	0.07	5	Simien & Prugniel (1997)
NGC 4450	2	43.9/2.8	45.0	126	0.25	10	Fillmore, Boroson & Dressler (1986)
NGC 4579	2	38.5/95.3	55.0	174	0.22	5–10	Palacios et al. (1997), Heraudeau & Simien (1998)
NGC 4596	0	44.3/116	45.0	149	0.15	5	Bettoni & Galletta (1997)
NGC 4643	0	33.3/50	79.6	167	0.1	5	Magrelli, Bettoni & Galletta (1992)
NGC 5005	3	63.6/67.9	110.0	213	0.25	5	Batcheldor et al. (2005)
NGC 7727	1	26.9/159.8	35.0	181	0.27	8	Simien & Prugniel (1997)
ESO 208-G21	−4	43.9/109	110.0	150	0.52	5	Carollo et al. (1993)

radius of $V_{\max}$. Therefore $V_{\max}/\sigma$ measures the importance of rotation in supporting the galaxy against its self-gravity.

In Table 1 we have collected the stellar kinematic observations from the literature for all those galaxies in our sample, mainly early-types, that have measurements along the major axis of the disc. We use the major axis position angles (PAs) and inclinations that we obtained by fitting elliptical isophotes to deep optical or near-infrared (near-IR) images using the 'ellipse' routine in IRAF. The 'PA' and the inclination 'INC' are shown in the table (cos INC = b/a, where b and a are the minor and major axis ratios). The bulge-dominated regions of the discs were evaluated, based on our structural decompositions: the bulge was taken to be inside the radius where the surface brightness of the bulge exceeds that of the disc (denoted as r in the table). $V_{\max}$ was then taken to be the maximum line-of-sight rotational velocity inside the bulge-dominated region. The ellipticities inside the bulge dominated region were taken from the radial ϵ profiles (ϵ in the table). The last column in Table 1 lists the references for the kinematic data. T in the first column is the Hubble-type index.

The data are shown in Fig. 4, where the diagonal curve represents an isotropic oblate–spheroid model taken from Binney (1978). In the early diagrams by Illingworth (1981), Kormendy (1982) and Davies et al. (1983) the elliptical galaxies and bulges of disc galaxies flattened by random velocities lie below the oblate line, whereas fast-rotating disc-like bulges are expected to appear above that line. The reliability of this approach has been recently verified theoretically by Binney (2005). As the apparent ellipticity and the maximum rotational velocity of the bulge depend also on galaxy inclination, models with different inclinations were calculated by Binney (2005). He showed that the inclination would shift the data points in the $V_{\max}/\sigma$ versus ϵ diagram almost parallel to the isotropic oblate rotator line. We find that 40 per cent of the S0 galaxies in our sample appear both above the line. Of the five galaxies that appear above

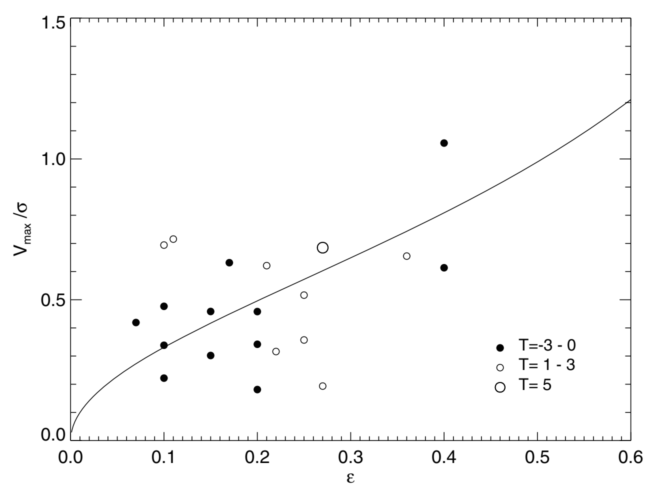

Figure 4. The kinematical properties of the bulges for a subsample of galaxies. $V_{\max}$ is the maximum line-of-sight rotational velocity of the bulge measured from the absorption lines, σ is the line-of-sight stellar velocity dispersion of the bulge just outside the nucleus, and ϵ is the characteristic ellipticity in the region interior to the radius of $V_{\max}$. The values are taken from our Table 1, and the different symbols represent different Hubble-type indexes. Inclination of the disc would shift the data points almost along the oblate rotator line, as predicted by the models of Binney (2005).

the line, one is non-barred and four have primary bars. Of the S0 galaxies below the line, five are barred and two are non-barred.

Our emphasis here is not to do any detailed interpretation of the kinematic data because this is done for early-type galaxies by Cappellari et al. (2005, 2007), based on modelling of 2D kinematic observations. However, the kinematic data for the galaxies in our sample indicate that many of the early-type galaxies are likely to be rotationally dominated. This is also consistent with the results obtained by Cappellari et al. for a sample of S0 galaxies. Following our definition of a pseudobulge in Section 3, both the inner component of the bar ("thick" component in Fig. 8, boxy/peanut in edge-on galaxies) and the nearly exponential central component could be pseudobulges.

5 BARS AND OVALS IN THE HUBBLE SEQUENCE

In this study our interests in the properties of bars stems from two reasons. First, we can try to evaluate whether the bar itself, or some part of it, could be a pseudo-bulge (as outlined in Section 3). In order to have a more consistent view of these pseudo-bulge candidates, we compare the Fourier properties of bars/ovals with the results obtained by the decompositions for the same galaxies. Secondly, by studying the properties of bars in the Hubble sequence and by comparing these properties with the predictions of dynamical models, we can evaluate how bars evolve in the Hubble sequence, if at all.

5.1 How prominent are bars?

In de Vaucouleurs' family classification (RC3) bars are divided into strong (B) and weak (AB) bars, based mainly on visual inspection of how prominent the bar looks in an optical *B*-band image, although the morphology of the bar also comes into the classification in the sense that bars typically classified as SAB often have more oval-like morphologies. In more recent works bars are generally characterized as 'strong' when they are *long* (relative to the scalelength of the disc) and *massive* (have large $m = 2$, 4 Fourier density amplitudes), and also when they *have large ellipticities* or the *tangential forces induced by bars are large*. As the orbital families of bars strongly depend on the underlying gravitational potential, one would expect a clear correlation between the ellipticity and the tangential force, which is indeed also found to be the case (Laurikainen, Salo & Rautiainen 2002; Buta et al. 2004).

There are many optical (Elmegreen & Elmegreen 1985; Martin 1995; Erwin 2005) and infrared (Regan & Elmegreen 1997; Laurikainen et al. 2002, 2004a) studies showing that bars in early-type spirals are longer than bars in late-type spirals. The estimation of bar length is not trivial (see Athanassoula 2005), but the different bar length estimates (visual inspection, maximum in the ellipticity profile, Fourier phase angle or the maximum in the force profile) seem to lead to a similar conclusion showing that bars in the early-type galaxies are longer. On the other hand, bars in early-type spirals are found to have smaller ellipticities (Martin 1995; Shlosman, Peletier & Knapen 2000; Laurikainen et al. 2002; Whyte et al. 2002; Laurikainen et al. 2004a) and smaller tangential forces (Laurikainen et al. 2002; Buta et al. 2004) than bars in late-type spirals.

In Fig. 5 we show four different bar strength indicators calculated for our sample of 216 galaxies: (1) Q_g, which is the maximum of relative tangential force in the bar region, normalized to the underlying mean axisymmetric force field, (2) the ellipticity of a bar using the f_{bar} index by Whyte et al. (2002), (3) the relative mass of a bar, as estimated from the $m = 2$ (A_2) and $m = 4$ (A_4) Fourier amplitudes in the bar region and (4) the length of a bar, as estimated from the phases of the A_2 amplitudes, normalized to the radial scalelength of the disc. For Q_g, A_2 and A_4, the values are collected from

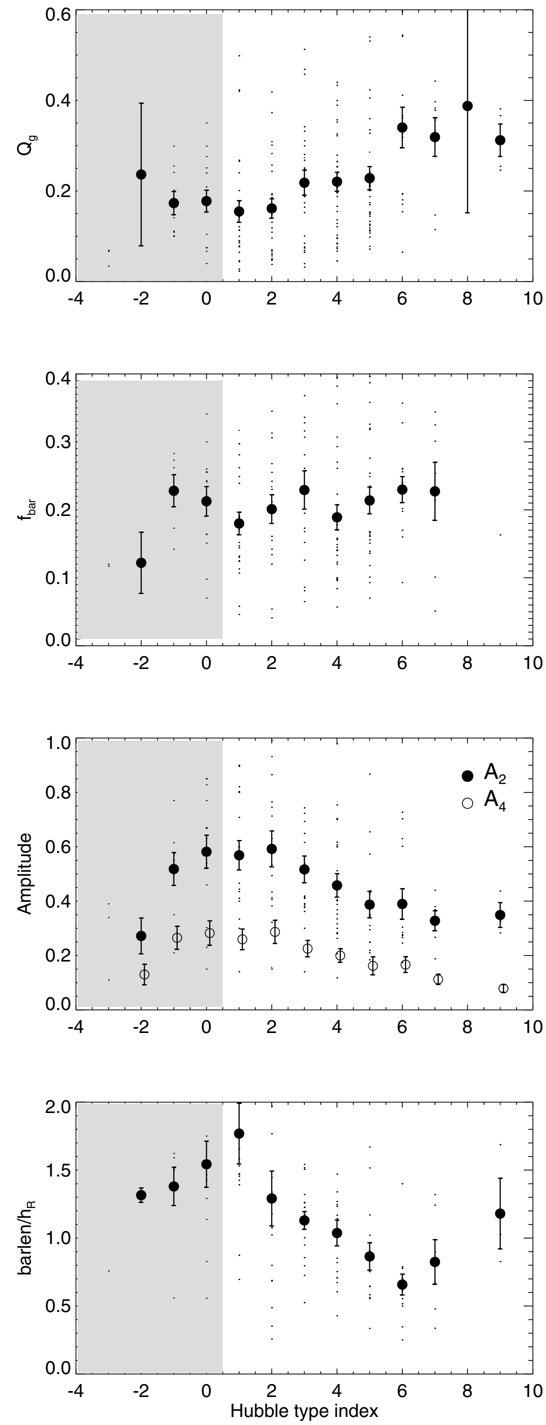

Figure 5. Four different estimates of bar strength are calculated for our sample of 216 galaxies and shown as a function of the Hubble-type index. Q_g denotes the bar-induced maximum tangential force normalized by the azimuthally averaged radial force. The parameter f_{bar} is a measure of the ellipticity of the bar, as defined by Whyte et al. (2002), and explained in more detail in the text. The A_2 and A_4 are amplitudes of density for the $m = 2$ and 4 Fourier modes (normalized to axisymmetric component). Bar length has been estimated from the phases of the A_2 Fourier amplitudes so that the length is the radial distance up to which the phase is maintained nearly constant in the bar region. The length is normalized to the scalelength of the disc, h_R, obtained from deep near-IR image.

Table 2. The ellipticies of the barred NIRS0s galaxies, using the parameter $f_{\rm bar}$ as defined by Whyte et al. (2002).

NGC	$f_{\rm bar}$
718	0.124
936	0.273
1022	0.281
1079	0.262
1317	0.107
1326	0.220
1350	0.234
1387	0.117
1415	0.239
1440	0.173
1452	0.297
1512	0.306
1533	0.167
1574	0.120
2273	0.249
2681	0.098
2781	0.070
2859	0.235
2983	0.262
3081	0.256
3358	0.132
3626	0.142
3941	0.077
4245	0.164
4340	0.283
4596	0.241
4608	0.243
4643	0.255

Laurikainen et al. (2004b, 2006a) and Laurikainen et al. (2005). The values of $f_{\rm bar}$ for the OSUBSGS sample are those derived by Whyte et al. (2002, see also Buta et al. 2004), whereas for the galaxies in the NIRS0S sample $f_{\rm bar}$ was calculated in this study using the formula given by Whyte et al. (see Table 2):

$$f_{\rm bar} = 2/\pi\ \{\arctan[(b/a)^{-1/2}] - \arctan[(b/a)^{+1/2}]\}, \quad (1)$$

where *b*/*a* is the minor-to-major axis ratio of a bar. We used *b*/*a* as derived from the maximum ellipticities in the bar region, obtained from our radial ϵ profiles, and corrected for the inclination of the disc (see Abraham et al. 1999). For completeness, we also estimated the lengths of the bars for some of the galaxies in the NIRS0S sample based on the phases of the Fourier amplitudes, in a similar manner as estimated previously by us for the other galaxies in our sample. The strength of this comparison is that all bar strength indicators are calculated for the same galaxies using the same homogeneous data base. The advantage of using IR images is well known: we are not missing bars that might be obscured by dust in the optical region, or where morphology might be masked by pockets of star formation.

In Fig. 5 we can look separately at the tendencies for the early (shaded region) and late-type (non-shaded region) galaxies. Characteristic for the spiral galaxies is that bars become *stronger* towards the later Hubble types when $Q_{\rm g}$ is concerned, and *weaker* when the length or the relative mass of a bar is concerned. These tendencies for spiral galaxies have been previously shown by Laurikainen et al. (2004a), and for $Q_{\rm g}$ also by Buta et al. (2004). Buta et al. (2005) also showed that in some cases spiral arms might affect the force ratio (in which case $Q_{\rm b}$ was used to denote the bar forces after subtraction

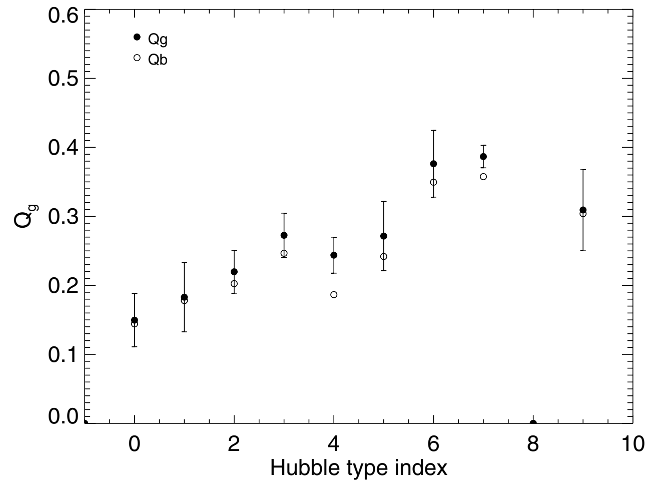

Figure 6. Comparison of the mean bar torques without ($Q_{\rm g}$, from Laurikainen et al. 2004b) and with ($Q_{\rm b}$, from Buta et al. 2005) the correction of the spiral arms in the OSUBGS sample. Only those galaxies are included for which it was possible to apply the bar/spiral separation approach.

of the spiral component before calculating the forces). However, in Fig. 6 we show that any superposition of spiral arms with bars does not significantly affect the tendency we find for $Q_{\rm g}$ in the Hubble sequence. For $f_{\rm bar}$ there might be a similar increase towards later types as for $Q_{\rm g}$, but it is not as clear: actually any possible variations in $f_{\rm bar}$ in the Hubble sequence are within the error bars. This is consistent with the result obtained by Marinova & Jogee (2006) who found that the ellipticity of a bar is practically independent of the Hubble type. In any case we find that $Q_{\rm g}$ is well correlated with $f_{\rm bar}$ when all morphological types are taken together (Fig. 7). This correlation exists also if $Q_{\rm b}$ is used, but in that case the dispersion is somewhat larger. For spiral galaxies the apparent controversy between the bar length and the relative mass of a bar in one hand, and $Q_{\rm g}$ on the other, has been discussed by Laurikainen et al. (2004a). They showed that although bars in the early-type spirals are longer and

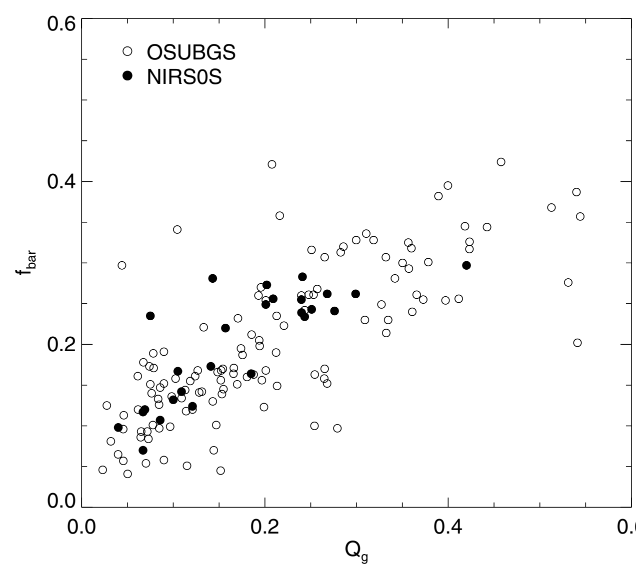

Figure 7. Correlation between the ellipticity of the bar, $f_{\rm bar}$ and the bar torque, $Q_{\rm g}$. The open circles show mainly the spiral galaxies, whereas the filled circles show the early-type galaxies

more massive, the bar-induced tangential forces are weaker relative to mean axisymmetric forces, because they are diluted by the more massive bulges in these systems.

Fig. 5 also shows that the trends we find for spiral galaxies do not extend to S0s, which might be an important clue for evaluating the evolutionary history of galaxies in the Hubble sequence. Bars in the early-type S0 galaxies are clearly shorter (see also Erwin 2005) and less massive than bars in the later type S0s or in S0/a galaxies. For $Q_{\rm g}$ and $f_{\rm bar}$ the opposite might be true, but the number of galaxies in our sample is too small to confirm that. While calculating $Q_{\rm g}$ the largest uncertainty is related to the assumed vertical thickness of the disc (Laurikainen & Salo 2002). We used a vertical thickness based on the empirical relation between the morphological type and the vertical thickness of the disc, as estimated by de Grijs (1998). Nevertheless, this uncertainty (see fig. 6, in Laurikainen et al. 2004b) is clearly smaller than the trend we find for $Q_{\rm g}$ in the Hubble sequence.

5.2 Fourier amplitude profiles of bars

In order to study a possible connection between bars and pseudo-bulges we compare the different structural components that we identify using the decomposition method and the Fourier analysis method for barred galaxies.

5.2.1 Early-type galaxies

The radial profiles of Fourier density amplitudes of 26 of the S0-S0/a galaxies in our sample have been previously studied by Buta et al. (2006). They showed that the A_2 amplitude profiles of bars can be fitted by Gaussian functions, using either single (SG), double (DG) or multiple (MG) Gaussian functions. In Buta et al. (2006), bars fitted by a double Gaussian function were found to have, on average, larger $Q_{\rm g}$ than bars fitted by a single Gaussian function. In the following we discuss the other bar strength indicators and the properties of bulges, as derived by the decomposition analysis, for the same galaxies. As the MG-type profiles are generally very complex we concentrate only on the SG- and DG-type bars in the following.

The mean parameters of bars and bulges for SG- and DG-type bars are collected to Table 3. We find that DG-type bars not only have larger values of $Q_{\rm g}$, but that they are also more elliptical, longer and more massive than SG-type bars. It appears that the strong DG-type bars have slightly less massive (have smaller B/T flux ratio) and more exponential bulges than the weaker SG-type bars. This indicates that the bar type is connected to the central exponential part of the surface brightness profile, which we have identified as a bulge in the decompositions. Both groups of galaxies (SG and DG) have similar absolute $K_{\rm s}$-band magnitudes, which eliminates the possibility that the differences we find were due to a magnitude bias.

Table 3. Comparison of galaxies having single (SG) and double (DG) Gaussian bars. The errors are standard deviations of the mean.

	SG	DG
$\langle M_K \rangle$	23.4 ± 0.2	23.4 ± 0.3
$\langle Q_{\rm g} \rangle$	0.09 ± 0.01	0.23 ± 0.03
$\langle f_{\rm bar} \rangle$	0.17 ± 0.09	0.22 ± 0.09
$\langle A_2 \rangle$	0.39 ± 0.03	0.61 ± 0.05
$\langle$bar length$/h_{\rm R}\rangle$	1.14 ± 0.11	1.56 ± 0.12
$\langle B/T \rangle$	0.27 ± 0.04	0.17 ± 0.02
$\langle n \rangle$	1.9 ± 0.2	1.4 ± 0.2

In order to understand better the SG and DG nature of bars, we picked up four characteristic examples of early-type galaxies and inspected their properties in more detail (see Figs 8 and 10). For identifying better the components both in the amplitude profile and in the decomposition plot the peaks from the Gaussian fitting to the A_2 amplitude profiles are also shown. The parameters for calculating these peaks were taken from Table 3 in Buta et al. (2006). The effective radius of the bulge (from the decomposition) is indicated by a white contour. NGC 3941 is a typical example of a galaxy with an SG-type bar. The maxima in the A_2, A_4 and A_6 amplitude profiles appear at the same radial distance, a behaviour which is characteristic for SG-type bars in general, though in some SG-type bars (like NGC 1440) the lower modes are slightly shifted towards smaller radial distances. NGC 3941 has two distinct amplitude maxima in the A_2 profile, the main maximum belonging to the primary bar, and the lower maximum (at $r < 5$ arcsec) to an inner disc. The radial $Q_{\rm T}$ profile follows the A_2 amplitude profile so that the two $Q_{\rm T}$ maxima appear nearly at the same radial distances as the two amplitude maxima. The bulge that we find in the decomposition is almost as extended as the bar, indicating that the bar and the bulge are separate components. SG-type profiles were found to appear both among the primary and the secondary bars, but all clearly identified secondary bars have SG-type amplitude profiles.

As defined by Buta et al. (2006), DG-type bars have a broad A_2 amplitude profile, of which category the galaxies NGC 4245, 2859 and 1452 are representative examples. NGC 4245 has two local density peaks (indicated as thick and thin lines in Fig. 8) both in the lower (A_2) and in the higher Fourier modes (A_4 and A_6). Again, the radial $Q_{\rm T}$ profile follows the A_2 amplitude profile: one can imagine that the broad maximum is actually a superposition of two partially overlapping $Q_{\rm T}$ peaks. In the structural decomposition the inner and outer components were fitted with two Ferrers functions with minor-to-major axis ratios of 0.2 and 0.7, respectively. Additionally, the galaxy has an exponential bulge (indicated also in the decomposition plot) with a Sersic index $n = 1.3$. This value is very similar to that obtained by Aguerri et al. (2005) for a sample of 14 barred S0 galaxies using a bulge/disc/bar decomposition. The flattening of the inner bar component (nearly in the same direction as the outer component) is higher than the value of 0.8–0.9 typically found for ovals (see KK2004). Also, higher Fourier modes are not expected in ovals. This leaves room for the interpretation that the two components in the A_2 profile belong to a single bar with thick and thin components (note that here we are discussing of a low-inclination galaxy and do not necessarily know about the vertical thickness of the bar). Following our definition of a pseudo-bulge in Section 3, both the inner component of the bar and the nearly exponential central component could be pseudo-bulges.

NGC 1452 also has a broad double peaked A_2 amplitude profile, but in this case the higher Fourier modes (A_4, A_6 and A_8) appear clearly only at $r \sim 35$ arcsec, which is the more distant component of the A_2 double peak. Also, the $Q_{\rm T}$ profile does not completely follow the A_2 amplitude profile: the peak in the $Q_{\rm T}$ profile is fairly sharp and occurs at the radial distance where the higher Fourier modes are also significant. This maximum evidently corresponds to a bar, a component which appears also in the surface brightness profile at a similar radial distance. The strongest A_2 maximum appears at $r \sim 20$ arcsec, where the higher Fourier modes are weak or absent. At this radial distance there is only a weak shoulder in the $Q_{\rm T}$ profile. Most probably this A_2 maximum corresponds to a bright oval, identified as such also in the structural decomposition.

NGC 2859 has a very broad A_2 amplitude profile, but in this case the higher Fourier modes appear only at small radial distances

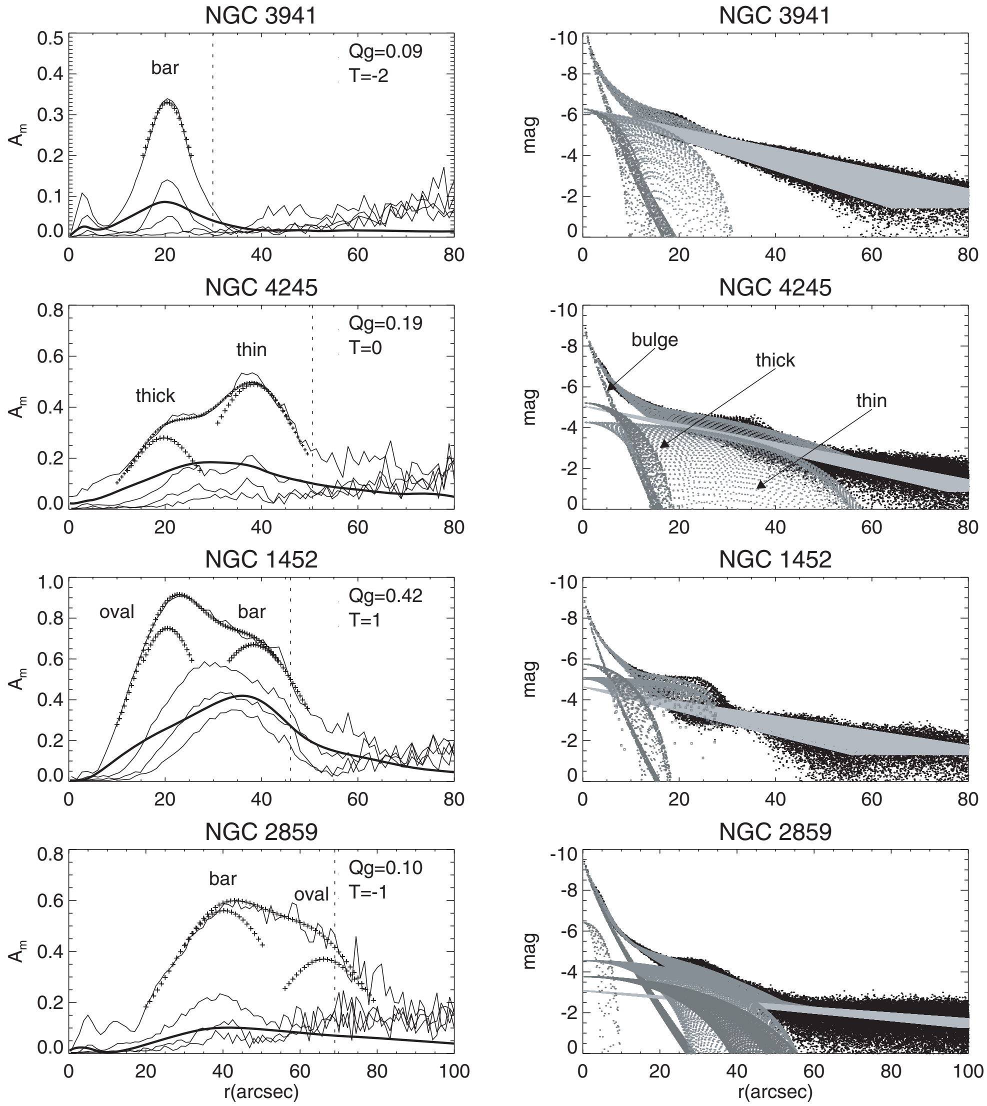

Figure 8. Examples of early-type disc galaxies in our sample. In the left-hand row are shown the Fourier amplitude profiles (thin lines) and the Q_T profiles (thick lines) for these galaxies. The crosses show simple double Gaussian fits to the A_2 profiles, for which fits the parameters were taken from Buta et al. (2006): shown separately are the two peaks and the overall fit to the observed profile. The vertical dashed line shows the length of the bar, estimated from the phases of the A_2 Fourier amplitudes. In the upper right-hand corners of these figures are indicated the values of the bar torques and the Hubble-type indexes. In the y-axis the density amplitudes A_m of each mode are shown (normalized to axisymmetric component). In the right-hand row of the figure are shown the results of the multicomponent decompositions for the surface brightness profiles for the same galaxies. The disc was fitted by an exponential function, the bulge by a Sersic function, and the bars typically by a Ferrers function and the ovals and inner components of bars by a Sersic function. A more detailed description of these decompositions can be found in Laurikainen et al. (2006a). 'Thin' and 'thick' lines refer to the two components of the bar.

($r \sim 40$ arcsec). The Q_T profile is extremely shallow showing only a modest peak at the radial distance where the higher Fourier modes are present ($r \sim 40$) arcsec. Our conclusion is that the A_2 profile is broad because the galaxy has a weak bar and a prominent oval extending outside the bar, a conclusion made also by Buta et al. (2006) for this galaxy. The outer oval has characteristics of a dispersed ring, and the bar appears inside a prominent lens having the same radius as the bar. The small peak in the A_2 amplitude profile at $r <$ 10 arcsec, visible also in the surface brightness profile and in the Q_T profile, corresponds to a secondary bar. Both NGC 1452 and 2859 have nearly exponential bulges with $n = 1.2$ and 1.3, respectively.

We conclude that the broad or double peaked A_2 amplitude profiles of bars in the early-type galaxies considered here correspond either to a two-component bar with a thick inner part and a thin outer part, or to a superposition of a bar and an oval (small or extended). Many of the DG-type bars we find in our sample are two-component bars. The DG-type bars were found to be stronger on average than the more simple SG-type bars, using all four bar strength indicators. We also find that strong bars typically have fairly sharp outer cut-offs in the A_2 profiles, in agreement with previous findings by Ohta (1996).

5.2.2 *Late-type galaxies*

We inspected the Fourier amplitude profiles also for all galaxies in the OSUBSGS sample, although due to the prominence of spiral arms the interpretation of these profiles is not always

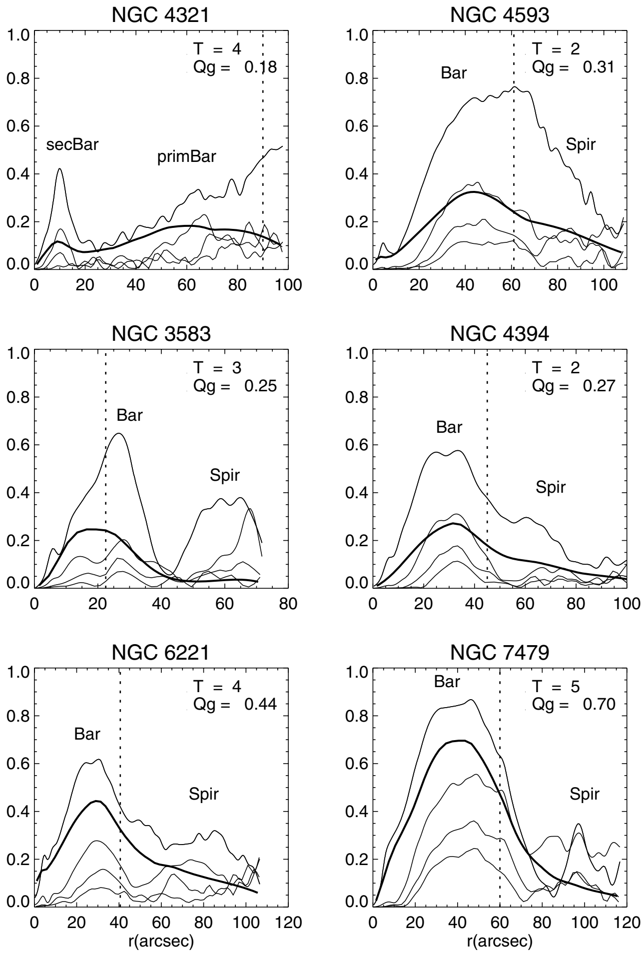

Figure 9. Characteristic examples of spiral galaxies in our sample. These figures are similar to those shown in the left-hand row in Fig. 7. The symbols are also the same as in Fig. 7.

straightforward. For this reason any quantitative comparison of SG-/DG-type bars in different Hubble-type bins was not possible. However, similar density profiles as found for the early-type galaxies are found also for the spirals.

Examples of characteristic SG- and DG-type profiles of bars in spiral galaxies are collected in Fig. 9. As in Fig. 8, the radial Q_T profiles and Fourier amplitude profiles are shown. The primary bar in NGC 4321 is weak and affected by the spiral arms and an aligned inner part which is well-defined in the near-IR (Knapen et al. 1995a,b). The morphological type is SAB(s)bc, but the SG-type amplitude profile of the bar is similar to those in any other morphological type: the A_2 density maximum is sharp and the higher Fourier modes A_4 and A_6 (even A_8 is present) are also significant. All modes appear nearly at the same radial distance, which is also the location of the Q_T maximum.

The five remaining galaxies in Fig. 9 are candidates of DG-type bars. NGC 3583 has clearly a two-component maximum at $r <$ 40 arcsec, both in the lower and in the higher Fourier modes, most probably indicating that the bar has both an inner and an outer component. The Q_T peak is also very broad. However, the phase of the A_2 component is maintained nearly constant only to $r \sim$ 25 arcsec, which suggests that the outer part of the bar has some spiral-like characteristics, evident also in the direct K_s-band image. The galaxies NGC 4394 and 7479 are more clear examples of two-component bars. The bars in these galaxies have similar double-peaked amplitude profiles both in the lower and the higher Fourier modes. The bar in NGC 4593 is also similar to those in NGC 4394 and 7479. The large A_2 maximum at $r \sim 70$ arcsec is caused by the prominent spiral arms starting at the two ends of the bar.

We find that although bars in spiral galaxies are less prominent than those in the early-type galaxies, strong bars in all morphological types have similar characteristics. Ohta, Hamabe & Wakamatsu (1990) were the first to indicate that the higher Fourier modes of bars are characteristic for early-type galaxies, but they also argued that these modes are absent in bars of spiral galaxies. However, we show that the higher Fourier modes are characteristic for *all* strong bars (see the Sc-type spiral galaxy NGC 7479 with $Q_g = 0.7$, and NGC 6221 with $Q_g = 0.44$). According to Ohta (1996) the early-type galaxies have sharp cut-offs in the amplitude profiles at the ends of the bar, although such cut-offs were argued to be missing in bars of late-type galaxies. Due to the strong spiral arms, the shapes of the amplitude profiles in spiral galaxies are difficult to evaluate. However, NGC 7479 is an example showing that strong bars even in late-type spirals, can have fairly sharp outer cut-offs in their A_2 profiles.

In the decompositions for barred galaxies we have generally interpreted as a bulge the nearly exponential innermost part of the surface brightness profile, whereas the "thick" middle component of the bar (in DG-type bars) was fitted by a separate Ferrers or Sersic function. While calculating the *B*/*T* flux ratio this "thick" middle component goes to the disc. However, we have tested (see Laurikainen et al. 2005) that the middle component does not affect the *B*/*T* flux ratio or the Sersic index *n*.

5.2.3 Bar morphologies in early- and late-type galaxies

The images of the early-type galaxies in Fig. 8 are shown in Fig. 10. The main observed bar morphologies in galaxies are the classical bar and the ansae-type bar, the latter having density condensations at the two ends of the bar. A typical example of a classical bar is that in NGC 1452, and of an ansae-type bar that in NGC 2859. The bar in NGC 4245 is also of weak ansae type morphology. Additionally x-shaped bars are detected in galaxies. We compared bar morphologies for the early (S0-S0/a) and late-type (later than S0/a) galaxies in our sample: we found that 40 per cent of the early-type galaxies have ansae-type morphologies, whereas ansae in spiral galaxies appear only in 12 per cent of the galaxies (14 ansae among 115 OSUBSGS galaxies).[3]

Other fairly flat components in galactic discs are the ovals and lenses, which in the dynamical models are generally considered as weak bars. We found that although ovals are not very common in spiral galaxies, even 70 per cent of S0-S0/a galaxies have either lenses or ovals. Some galaxies, like NGC 1411, seem to be dominated by a superposition of a series of lenses (see Buta et al. 2007), to such a degree that it is difficult to say whether these galaxies have any other structural components at all. Our future analysis will show other similar examples (to appear in a forthcoming paper). Prominent lenses are generally manifested as multiple exponentials in the surface brightness profiles (see Laurikainen et al. 2006a). The lenses/ovals appear both in barred and in non-barred galaxies. In barred galaxies the lenses typically surround bars having the same radial extent with the bar (like the inner lens in NGC 2859), but they

[3] A similar result for the early-type galaxies has been obtained also by Martinez-Valpuesta, Knapen & Buta, private communication.

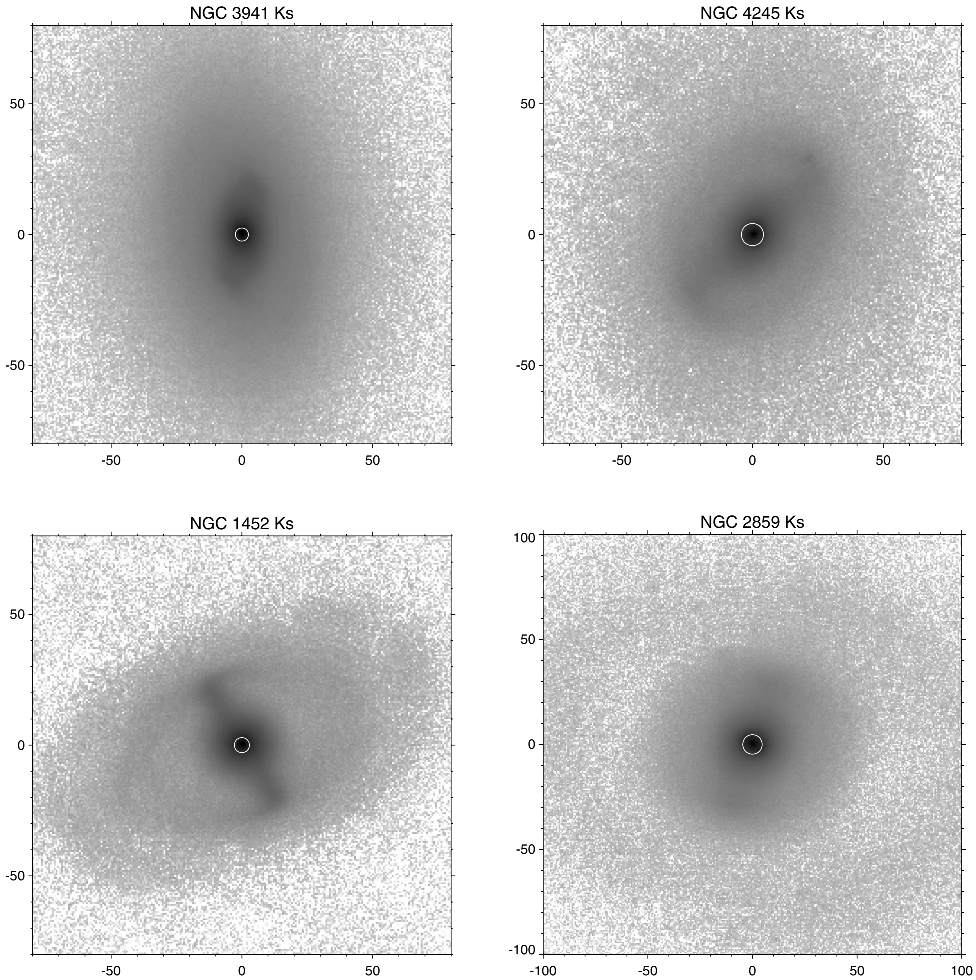

Figure 10. The images of the galaxies of Fig. 8 are shown in a logarithmic scale in the sky plane. The north is up and east is towards the left-hand side. The *x*- and *y*-axes are given in arcseconds. Note that the nearly exponential (pseudo-)bulge in barred early-type galaxies is generally the small roundish central component: in the figure the white circle indicates the effective radius $r_{\rm eff}$ of the fitted bulge. NGC 4245 has also a nuclear ring in the region of the pseudobulge.

can extend also to radial distances larger than the radius of the bar (like the outer oval in NGC 2859). Also, an oval coexisting with a normal bar may be aligned or misaligned with the bar, like the outer oval in NGC 2859 (see also Buta et al. 2006, 2007).

6 DISCUSSION

6.1 Nature of bulges in the Hubble sequence

In the hierarchical clustering model of the Universe dominated by cold dark matter (White & Rees 1978; Steinmetz & Navarro 2002) the dominant mechanism for producing bulges is by mergers of disc galaxies. Mergers of equal-mass galaxies yield remnants with properties similar to those found in elliptical galaxies (Barnes 1988; Hernquist 1993; Lima-Neto & Combes 1995; Balcells & Gonzalez 1998). However, a problem with these models is that the bulges in spiral galaxies and, as discussed in this study, even in early-type disc galaxies do not resemble elliptical galaxies. Nevertheless, it is not clear how strict the criterion for the merger origin is: there is recent evidence based on the cosmological dynamical models by Springel & Hernquist (2005) that if sufficient gas remains following a major merger, cooling can quickly reform the disc. This yields remnants that are closer to spiral galaxies, both structurally and kinematically. However, detailed comparisons between observations and model predictions are not yet possible.

There is strong evidence showing that the bulges in spiral galaxies are predominantly pseudo-bulges formed by star formation in the disc (see the review by KK2004). This is particularly clear for spiral galaxies of type Sb and later, which show bulges that are largely exponential, and whose relative bulge masses are small enough to be explained by the observed gas masses in galactic discs. Also, for spiral galaxies the relative mass of the bulge increases with the galaxy's luminosity. Although this is not straightforward to interpret, it is consistent with the view that the bulges were formed by star formation in the disc. Luminous galaxies have more differential rotation and shear than lower luminosity galaxies, thus leading to enhanced star formation in the disc, which can eventually be converted to the mass of the bulge. But the *B*/*T* flux ratio can increase also because of spreading of the outer disc due to the angular momentum transport in the disc (Lynden-Bell & Kalnajs 1972; Tremaine 1989), which would cause an apparent increase in the *B*/*T* flux ratio (see KK2004). That pseudo-bulges in spiral galaxies form by star formation in the disc is supported also by recent *Spitzer Space Telescope* observations by Fisher (2006) who showed that galaxies which are structurally identified as having pseudo-bulges have higher central star formation rates than galaxies having classical bulges. Bars may help in transferring the gas towards the central regions of the galaxies, but they are not a necessary requirement for central gas accumulation to occur (Sakamoto et al. 1999; Sheth et al. 2005). It has been suggested by Zhang (1998) and Zhang & Buta (2007) that, unlike in Lynden-Bell & Kalnajs (1972), secular torque action may be operating also in the stellar component.

The predominance of old stellar populations and the de Vaucouleurs-type surface brightness profiles in the early-type disc galaxies are generally used to claim that their bulges are merger-built structures (e.g. Schweizer 2005). KK2004 suggested that this might be the case for most S0-Sb type galaxies. However, we have shown that the bulges also in S0-Sb galaxies largely have characteristics of pseudo-bulges: the mean Sersic index $\langle n \rangle < 2$, and 56 per cent of these galaxies in our sample have nuclear bars, nuclear rings or central discs in the region of the bulge. These kinds of structures are not possible to form in hot bulges, dominated by random motions of stars. The obtained fairly low B/T flux ratios ($\langle B/T \rangle < 0.35$) in these galaxies are also consistent with the pseudo-bulge interpretation. Some of the galaxies also have kinematic evidence of pseudo-bulges. Rotationally dominated inner discs have been previously found also by Erwin et al. (2003) for two S0 galaxies, and by Cappellari et al. (2005, SAURON) for a sample of S0s, using high-resolution integral field spectroscopy. Cappellari et al. found that the bulges in most S0s galaxies are fast-rotating systems. All these observations contradict the view according to which a large majority of bulges in S0 galaxies were formed by mergers of disc galaxies in the distant past.

Alternatively, S0 galaxies have been suggested to be former spirals stripped of gas (Dressler et al. 1997), in which case the pseudo-bulges we find in the early-type galaxies could be formed by star formation in the disc in a similar manner as in spiral galaxies. A problem with this scenario is that spiral galaxies do not have sufficient gas to build up masses of bulges that typically consist of 30 per cent of the total galaxy mass. However, it has been discussed by Athanassoula (2005) that bars can induce formation of pseudo-bulges, not only by adding more mass to the bulge by star formation, but also by redistributing stellar matter due to the evolution of stellar orbital families of bars. In order to elaborate this view, the internal dynamical evolution of bars will be discussed in the following.

6.2 Internal evolution of bars

The evolution of stellar bars is affected by dynamical instabilities leading to long-term changes in their morphologies. When a bar forms in numerical simulations it is thin, but soon develops a vertically thick inner part and a disk-like, more extended middle component, generally associated with the boxy/peanut structure observed in edge-on galaxies (Athanassoula & Misioritis 2002; Athanassoula 2005). In the simulation models the surface brightness profile on the inner component of the bar is nearly exponential, whereas the middle component is fairly flat (Athanassoula & Misioritis 2002, their Fig. 5). Based on our observational criteria for pseudo-bulges in Section 3, both components can be interpreted as pseudo-bulges.

In dynamical models the boxy/peanut structure is formed by the so-called buckling instability (Combes et al. 1990; Pfenniger & Friedli 1991; Raha et al. 1991; Berentzen et al. 1998; Athanassoula & Misioritis 2002; Athanassoula 2002, 2003; O'Neil & Dubinski 2003; Martinez-Valpuesta & Shlosman 2004; Athanassoula 2005; Debattista et al. 2005, 2006; Martinez-Valpuesta et al. 2006), where the orbital families of bars are changed in such a manner that a vertical thickening of the bar results. In recent studies (Athanassoula 2006; Martinez-Valpuesta et al. 2006) multiple buckling effects have also been discussed. Buckling is expected to be a natural part of the evolution of bars, of particular importance in strong bars. The presence of boxy/peanut structures in edge-on galaxies has previously been shown both kinematically (Kuijken & Merrifield 1995; Chung & Bureau 2004) and using surface photometry (Lütticke, Dettmar & Pohlen 2000; Bureau et al. 2006). Lütticke, Dettmar & Pohlen (2000) found that 54 per cent of all morphological types among edge-on galaxies have boxy/peanut bulges, which implies that they should be common also among the less inclined galaxies. However, detecting boxy/peanut structures in less inclined galaxies is difficult mainly because different parts of bars are seen in face-on and in edge-on views. This has been demonstrated by Athanassoula & Beaton (2006), who showed for M31 that although the boxy/peanut structure is visible at an inclination of 77°, it is shorter at this inclination than it is in the edge-on view. Also, in the face-on view the boxy/peanut structure is barely visible. Similar boxy/peanut structures as seen in M31 are visible also in other non edge-on barred galaxies like NGC 7020, 1527, 4429 and IC 5240 (Buta et al. 2007). Based on visual inspection alone the connection between these features and bars is clear in only two of these cases.

We find that although S0-S0/a galaxies in general have fairly exponential bulges, the bulge profiles are even more exponential for the barred S0-S0/a galaxies. Within these morphological types, barred galaxies also have slightly smaller B/T flux ratios than the non-barred galaxies. As bars are important drivers of gas to the central regions of galaxies, this observation does not fit the scenario where the bulges were formed solely by star formation in the disc by adding more mass to the bulge. Therefore, a more likely interpretation would be that the bulges in the barred early-type galaxies are a combination of secularly induced star formation and inner concentrations of bars. In this view it would also be natural to understand why so many S0s galaxies have nuclear rings: S0 galaxies are not completely deficient of gas, and bars can transfer the gas to the central regions of the galaxies where nuclear rings form. In case that the bulge is part of the disc these rings can appear also inside the bulge region.

We find many bars that in the K-band image look as having a thin (or slim) outer component and a thicker and shorter (or fat) inner component, nearly aligned with the outer bar component. This kind of bars were found to have double Gaussian Fourier amplitude profiles (DG-type bars), in contrast to bars that can be fitted by a single Gaussian (SG-type bars). These bars resemble morphologically the boxy/peanut bars. However, taking into account the difficulties in identifying them in dynamical models for less inclined galaxies, we cannot for sure associate them to buckling instabilities that produce similar structures. In the theoretical models, boxy/peanut structures are strongest in strong evolved bars (Athanassoula & Misioritis 2002). We found that also DG-type bars are on average considerably stronger than the SG-type bars ($\langle Q_g \rangle = 0.23$ and 0.09, and $\langle A_2 \rangle = 0.61$ and 0.39, respectively). In our structural decomposition we have added the flux of the thick component to the disc, but giving it to the bulge would not change our conclusions on the B/T flux ratios or the values of Sersic index.

6.3 Angular momentum transfer and the evolution of bars in the Hubble sequence

In modern dynamical models (Athanassoula 2003) bars evolve due to angular momentum transfer between the bar and the halo, which occurs near the resonances: disc material at the inner Lindblad resonance will lose angular momentum, while halo material near corotation and near the outer Lindblad resonance will absorb it.

How strong this angular momentum exchange is depends critically on the mass of the halo and its central concentration, the amount of mass near the resonances, and how dynamically cool or hot the disc and the halo are. Athanassoula (2003) reports three different ways bars can lose angular momentum: (1) by trapping particles outside the bar into elongated orbits of the bar, a process in which angular momentum is lost from the inner parts of the disc, while the bar becomes longer, (2) part or all of the orbits trapped in the bar become more elongated and the bar becomes thinner and (3) bars lose rotational energy, leading to a slow bar. These three processes are expected to be linked, so that due to strong angular momentum transfer *bars simultaneously become longer, thinner and more slowly rotating*. Athanassoula's models (2003) have also shown that *while bars become longer, their relative masses also increase*. These trends have been verified by other self-consistent 3D simulation studies like those made by Martinez-Valpuesta, Shlosman & Heller (2006). The first indication that bars grow when they evolve over time comes already from dynamical models by Sellwood (1980).

We can then look at how observations fit this scenario. Our observations show that bars become longer (when scaled to the scale-length of the disc) and more massive (as estimated from $m = 2$ Fourier amplitudes of density) from the late-type spirals towards the early-type spirals. These results are consistent with the evolutionary models by Athanassoula (2003) if the dark matter haloes or the bulges in the early-type spirals are more massive or more centrally concentrated than those in the late-type spirals. This process can be faster or slower, depending on the properties of the haloes. Taking into account that the relative masses of the bulges are fairly small in all morphological types, haloes might play a more important role in this process.

However, at odds with the model predictions, our analysis also shows that bars do not have larger Q_g values or larger ellipticities (f_{bar}) towards the early-type spirals. This behaviour of Q_g and f_{bar} should not necessarily be taken as a counterargument to the model predictions. This is because Q_g is diluted by the underlying axisymmetric component, generally the bulge, which is more massive in the early-type galaxies. Generally this is not taken into account in the simulations. It would be interesting if the simulations could confirm whether the opposite trends among the different bar strength indicators in the Hubble sequence is completely a dilution effect, as suggested by Laurikainen et al. (2004a), or whether it is related to the different mechanisms of how bars lose their angular momentum.

An additional verification for the hypothesis that bars evolve because they lose angular momentum would be to show that long, evolved bars are more slowly rotating systems than shorter and less evolved bars. However, this has been difficult to prove, partly because of the difficulties to measure the bar pattern speed, Ω_p. So far, Ω_p has been measured directly using the Tremaine–Weinberg method for some S0 galaxies (Merrifield & Kuijken 1995; Aguerri, Debattista & Corsini 2003; Corsini, Debattista & Aguerri 2003; Gerssen, Kuijken & Merrifield 2003; Debattista & Williams 2004; Rand & Wallin 2004), and only for two spiral galaxies (Gerssen et al. 2003). These direct measurements of Ω_p have repeatedly pointed to fast bars in early-type galaxies, contrary to what one would expect for evolved bars. The largest collection of Ω_p measurements for spiral galaxies comes from the 2D sticky particle simulation (Salo et al. 1999) models for 38 spiral galaxies in the OSUBSGS sample by Rautiainen, Salo & Laurikainen (2005) and Salo et al. (2006), who showed that the *bars in late-type spirals are actually slower rotators than bars in early-type spirals*. A similar trend has been found also by Zhang & Buta (2007) for 36 OSUBSGS sample galaxies using the potential–density phase shift method. It seems that both direct and indirect estimates of Ω_p show the opposite trend in the Hubble sequence, compared to that predicted by present simulation models.

Dark matter haloes are key issues in the dynamical models. It was shown by Persic, Salucci & Stel (1996), based on a large sample of rotation curve measurements, that the relative halo mass depends on galaxy luminosity so that galaxies with lower luminosities have relatively more massive dark matter haloes. This means that late-type spirals, dominated by low-luminosity galaxies, should have more massive dark matter haloes, and consequently also slower bars. There is also some direct observational evidence that the haloes in S0 galaxies might be smaller than in spiral galaxies (see the reviews by Romanowsky 2004, 2006). That would naturally explain the observation of fast bars in S0s, but then it would be difficult to understand the other properties of bars in these galaxies, like the relative masses or lengths of bars, properties which hint at evolved systems. Also, in the study by Rautiainen et al. (2005), low Ω_p values were found already for galaxies with Hubble types Sb-Sbc, which in this study were shown to have similar absolute K_s-band magnitudes as the earlier Hubble types. Therefore, the mass of the dark matter halo alone is not sufficient to explain the behaviour of Ω_p. It seems that there does not yet exist any coherent picture where all the observed properties of bars could fit with the predictions of the dynamical models.

If bulges were more important than haloes for the angular momentum transfer between the bar and the spheroidal component, then it would naturally explain the evolution of bars towards the early-type galaxies: although the bulges are on average fairly small in all Hubble types, they are still clearly more massive in the early-type galaxies. But again, fast bars in S0s would be a problem. This view also makes the assumption that S0 galaxies have relatively massive pre-existing bulges that trigger the evolution of bars. However, this assumption does not fit to the scenario where pseudo-bulges in barred S0 galaxies are largely part of the bar that develops during the evolution of the bar.

Interestingly, the growth of bars does not continue among the S0 galaxies, more likely, bars become weaker from S0/a galaxies towards the early-type S0s. This is not expected in the evolutionary models by Athanassoula (2003) if haloes are similar in these galaxies and are the driving force for the evolution. If bulges were the driving force for this behaviour, and the bulges were merger-built structures, it would be difficult to understand why also the *B*/*T* flux ratio behaves in a similar manner as bar strength. One would also expect the masses of the merger-built bulges to be independent of the subtype of S0, and particularly not to decrease towards the earlier types. A more likely explanation, capable of explaining the behaviour of both the bar strength and the *B*/*T* flux ratio, is based on the mechanism described by Athanassoula, Lambert & Dehnen (2005). They showed that if central mass concentrations, like realistic secondary bars or nuclear discs, are used in the models, bars become shorter, less massive and faster than in models without these centrally concentrated mass components. If bulges in early-type barred galaxies were largely part of the bar, as suggested by us, this mechanism would naturally explain why also the *B*/*T* flux ratio decreases towards early-type S0s: namely weak bars have also weaker central mass concentrations. Indeed, nuclear bars and inner discs appear in more than 50 per cent of the studied S0-S0/a galaxies in our sample. Ultimately, the efficiency of nuclear bars and discs in redistributing matter in the disc is related to the problem of cuspy haloes: if the haloes are cuspy as assumed in present cosmological models, the central parts of the galaxies are halo dominated, thus reducing the effects discussed by Athanassoula et al. (2005).

A completely different view of the evolution of bars in spiral galaxies has been presented by Bournaud & Combes (2002), who suggest that in the presence of continuous accretion of external gas bars become fairly short-lived systems, so that bars are recurrently formed and destroyed. In principle this is possible, but our observations do not shed any new light on this issue. The recent simulations by Debattista et al. (2006) suggest that bars are actually fairly robust systems so that high gas masses are required to destroy the bars. Somewhat smaller gas accretion are needed to destroy bars in the simulation models by Hozumi & Hernquist (2005), Bournaud, Combes & Semelin (2005) and Athanassoula et al. (2005).

6.4 Summary: proposed picture for the formation of bulges in the Hubble sequence

Properties of bars and bulges in the Hubble sequence are discussed, based on an analysis of 216 disc galaxies, selected from the OSUBSGS and NIRS0S samples. Our main emphasis has been to combine the various properties of bars and bulges, presented for the individual galaxies in a series of papers by us, and to discuss the implications of these measurements in the Hubble sequence. The properties of bars were derived mainly by Fourier techniques and the properties of bulges by applying a multicomponent decomposition code. The analysis results were compared with various dynamical models in the literature.

The picture that we propose as a result of this fairly comprehensive study is the following.

(1) *Bulges in spiral galaxies having morphological types Sb and later* are pseudo-bulges, largely formed by star formation in the central regions of the discs. For galaxies with $B/T < 0.1$ all bulges were formed this way. Pseudo-bulges are formed both in luminous and in less luminous galaxies. Bars can make the processes faster and more efficient, but they are not a necessary requirement for that.

(2) *Bulges in earlier Hubble types (S0$^-$-Sab)* are mainly pseudo-bulges, although classical bulges also appear among these galaxies. Bulges in barred and non-barred early-type galaxies might have physically different origins. Particularly in strongly *barred early-type galaxies* bulges are disk features formed both by secular star formation and by redistribution of disk material due to the orbital families of bars. Strong bars typically have also a fatter middle component with boxy isophotes, which can be interpreted as a pseudo-bulge as well. In *non-barred early-type galaxies* bulges can be classical bulges, or pseudo-bulges formed in a similar manner as in barred galaxies, but triggered by ovals or lenses (70 per cent of all S0-S/a galaxies have ovals/lenses). Superposition of a classical and a pseudo-bulge is also possible.

(3) According to theoretical models strong bars have both an exponential inner bar component, and a vertically thickened middle component of the bar. By definition, both components are considered as pseudo-bulges. In edge-on view both components are visible, but in less inclined galaxies the middle component does not look boxy anymore, and disappears in face-on view. This kind of bar can appear in all morphological types, but because bars are stronger in the early-type galaxies, they are expected to be more common in the early-type galaxies.

(4) Bars can make pseudo-bulges in two different ways: (i) by triggering gas infall to the central regions of the galaxies, thus leading to a growth of a pseudo-bulge (dominant in spiral galaxies) and (ii) by redistributing stellar material in the disc through the orbital families of bars (dominant in early-type disc galaxies). The stellar dynamical processes of bars are more important in the early-type galaxies, because bars in these systems are more evolved and stronger than in the later type systems.

(5) In the earliest type disc galaxies (S0$^-$-S0$^{\rm o}$) the nuclear bars and nuclear discs affect the dynamical processes so that bars start to become weaker (using all bar strength indicators). The pseudo-bulges, which are largely part of the bar, are then also expected to decrease in mass.

The observations that fit to this picture are the following.

Bars get stronger and more evolved towards the early-type galaxies: bars become longer and more massive, 90 per cent of the bars in the early-type galaxies have flat or intermediate-type surface brightness profiles (in comparison to largely exponential profiles in spirals), and 40 per cent of them have ansae-type morphologies (in comparison to 12 per cent in spiral galaxies). The fact that $Q_{\rm g}$ is smaller in the early-type systems can be explained by dilution of the tangential forces by the more massive bulges in these galaxies. The flat bar surface brightness profiles for early-type galaxies were first reported by Elmegreen & Elmegreen (1985).

If pseudo-bulges in barred early-type galaxies are largely part of the bar, as suggested by us, then it would explain the following.

(i) Why it is possible to detect pseudo-bulges even in the early-type galaxies having bulge masses larger than those that can be made by star formation in the disc alone in any of the Hubble types.

(ii) Why *B*/*T* flux ratios in barred early-type galaxies are smaller (and not larger) than in the non-barred early-type galaxies (increasing the bulge mass by star formation would be particularly efficient in barred galaxies which can easily convert the gas in the outer disc to the central regions of the galaxies).

(iii) The appearance of disc-like fine structures like nuclear rings in the region of the bulge even in the early-type galaxies is natural if the bulges are part of the disc.

What remains to be explained is the observed behaviour of the bar pattern speed in the Hubble sequence. It seems that the properties of the halo (mass or its central concentration) alone are not sufficient to solve this problem. The frequently detected lenses that often appear simultaneously with bars in galaxies, is something that has hardly been studied yet. It is still possible that some of the early-type galaxies are stripped spirals, of which NGC 1411 is an example: it is an S0 galaxy having a similar *B*/*T* flux ratio as Sc-type spirals. This particular galaxy belongs to a cluster, but other similar examples need to be studied.

ACKNOWLEDGMENTS

We wish to thank Lia Athanassoula, John Kormendy, Alfonso Aguerri, Inma Martinez-Valpuesta and the anonymous referee for valuable comments on this manuscript. All of them have considerably improved the manuscript. We also thank Anna Mäkinen for collecting the kinematic data from the literature, which made as a summer work in the Astronomy Division, University of Oulu. The support from the Academy of Finland is acknowledged. RB acknowledges the support of NSF Grant AST-0507140.

REFERENCES

Abraham R. G., Merrifield M. R., Ellis R. S., Tanvir N. R., Brinchmann J., 1999, MNRAS, 308, 569
Aguerri J. A. L., Debattista V. P., Corsini E. M., 2003, MNRAS, 338, 465
Aguerri J. A. L., Alias-Rosa N., Corsini E. M., Munoz-Tunon C., 2005, A&A, 434, 109
Andredakis Y. C., Sanders R. H., 1994, MNRAS, 267, 283

Andredakis Y. C., Peletier R. F., Balcells M., 1995, MNRAS, 275, 874
Athanassoula E., 2002, ApJ, 569, 83
Athanassoula E., 2003, MNRAS, 341, 1179
Athanassoula E., 2005, MNRAS, 358, 1477
Athanassoula E., 2006, in Wada K., Combes F., eds, Mapping the Galaxy and Nearby Galaxies. Ishigaki, Japan, preprint (astro-ph/10113)
Athanassoula E., Beaton R. L., 2006, MNRAS, 370, 1499
Athanassoula E., Misioritis A., 2002, MNRAS, 330, 35
Athanassoula E., Lambert J. C., Dehnen W., 2005, MNRAS, 363, 496
Balcells M., Gonzalez A. C., 1998, ApJ, 505, L109
Balcells M., Graham A. W., Dominiguez-Palmero L., Peletier R. F., 2003, ApJ, 582, L79
Balcells M., Graham A. W., Peletier R. F., 2004, preprint (astro-ph/0404379)
Barnes J. E., 1988, ApJ, 331, 699
Batcheldor D. et al., 2005, ApJS, 160, 76
Bell E. F., de Jong R. S., 2001, ApJ, 550, 212
Benson A. J., Frenk C. S., Sharples R. M., 2002, ApJ, 574, 104
Berentzen I., Heller C. H., Shlosman I., Fricke K. J., 1998, MNRAS, 300, 49
Bertin G. et al., 1994, A&A, 292, 381
Bettoni D., Galletta G., 1997, A&AS, 124, 61
Bettoni D., Galletta G., Vallenari A., 1988, A&A, 197, 69
Binney J., 1978, MNRAS, 183, 501
Binney J., 2005, MNRAS, 363, 937
Bournaud F., Combes F., 2002, A&A, 392, 83
Bournaud F., Combes F., Semelin B., 2005, MNRAS, 364, L18
Bosma A., 2003, IAU Symp., Rev MexAA, 17, 15
Bureau M., Athanassoula E., 2005, ApJ, 626, 159
Bureau M., Aronica G., Athanassoula E., Dettmar R. J., Bosma A., Freeman K. C., 2006, MNRAS, 370, 753
Buta R., Laurikainen E., Salo H., 2004, AJ, 127, 279
Buta R., Vasylyev S., Salo H., Laurikainen E., 2005, AJ, 130, 506
Buta R., Laurikainen E., Salo H., Block D., Knapen J., 2006, AJ, 132, 1859
Buta R., Corwin H., Odewahn S., 2007, The de Vaucouleurs Atlas of Galaxies. Cambridge Univ. Press, Cambridge
Caon N., Cappaccioli M., D'Onofrio M., 1993, MNRAS, 265, 1013
Cappellari M. et al., 2005, Nearly Normal Galaxies in a LCDM Universe. A conference celebrating the 60th birthdays of George Blumenthal, Sandra Faber and Joel Primack. UC Santa Cruz, Santa Cruz
Cappellari M. et al., 2007, MNRAS, 379, 418
Carollo C. M., Danziger I. J., Buson L., 1993, MNRAS, 265, 553
Carollo C. M., Danziger I. J., 1994, MNRAS, 270, 523
Carollo C. M., Stiavelli M., de Zeeuw P. T., Mack J., 1997, AJ, 114, 2366
Carollo C. M., Stiavelli M., Mack J., 1998, AJ, 116, 68
Carollo C. M., Ferguson H. C., Wyse R. F., G., 1999, The Formation of Bulges. Cambridge Univ. Press, Cambridge
Carollo C. M., Stiavelli M., Seigar M., de Zeeuw P. T., Dejonghe H., 2002, AJ, 123, 159
Chung A., Bureau M., 2004, ApJ, 127, 3192
Combes F., Debbash F., Friedli D., Pfenniger D., 1990, A&A, 233, 82
Corsini E. M. et al., 1999, A&A, 342, 671
Corsini E. M., Pizzella A., Bertola F., 2002, A&A, 382, 488
Corsini E. M., Debattista V. P., Aguerri J. A. L., 2003, ApJ, 599, L29
Cowie L. L., Songaila A., Hu E. M., 1996, AJ, 112, 839
Davies R. L., Efstathiou G., Fall S. M., Illingworth G., Schechter P. L., 1983, ApJ, 266, 41
Debattista V. P., Williams T. B., 2004, AJ, 605, 714
Debattista V. P., Carollo C. M., Mayer L., Moore B., 2005, ApJ, 628, 678
Debattista V. P., Mayer L., Carollo C. M., Moore B., Wadsley J., Quinn T., 2006, ApJ, 645, 209
de Grijs R., 1998, MNRAS, 299, 595
Denicolö G., Terlevich R., Terlevich E., Forbes D. A., Terlevich A., Carrasco L., 2005, MNRAS, 356, 1440
de Souza R. E., Gadotti D. A., dos Anjos S., 2004, ApJS, 153, 411
de Vaucouleurs G., de Vaucouleurs A., Corwin H. G. Jr, Buta R., Paturel G., Fouque P., 1991, Third Reference Catalogue of Bright Galaxies. Springer-Verlag, New York (RC3)
Dressler A. et al., 1997, ApJ, 490, 577
Elmegreen B., Elmegreen D., 1985, ApJ, 288, 438
Erwin P., 2005, MNRAS, 364, 283
Erwin P., Belträn J. C. Vega, Graham A. W., Beckman J. E., 2003, ApJ, 597, 929
Eskridge P. B. et al., 2002, ApJS, 142, 73
Faber R. E., Jackson R. E., 1976, ApJ, 204, 668
Falcön-Barroso J., Balcells M., Peletier R. F., Vazdekis A., 2003, A&A, 405, 455
Falcön-Barroso J. et al., 2004, MNRAS, 350, 35
Fillmore J. A., Boroson T. A., Dressler A., 1986, ApJ, 302, 208
Fisher D., 1997, AJ, 113, 950
Fisher D. B., 2006, ApJ, 642, L17
Fukugita M., Hogan C. J., Peebles P. J. E., 1998, ApJ, 503, 518
Gardner J. P., Sharples R. M., Frenk C. S., Carrasco B. E., 1997, ApJ, 480, L99
Gerssen J., Kuijken K., Merrifield M. R., 2003, MNRAS, 345, 261
Graham A. W., 2001, AJ, 121, 820
Haynes M. P., Jore K. P., Barrett E. A., Broeils A. H., Murray B. M., 2000, AJ, 120, 703
Heraudeau Ph., Simien F., 1998, A&AS, 133, 317
Heraudeau Ph., Simien F., Maubon G., Prugniel Ph., 1999, A&AS, 136, 509
Hernquist L. E., 1993, ApJ, 409, 548
Hozumi S., Hernquist L., 2005, PASP, 57, 719
Illingworth G., 1977, ApJ, 218, L43
Illingworth G., 1981, in Fall S. M., Lynden-Bell D., eds, Structure and Evolution of Normal Galaxies. Cambridge Univ. Press, Cambridge, p. 27
Jarvis B. J., Dubath P., Martinet L., Bacon R., 1988, A&AS, 74, 513
Jore K. P., Broeils A. H., Haynes M. P., 1996, AJ, 112, 438
Kent S. M., 1986, AJ, 91 1301
Knapen J. H., Beckman J. E., Heller C. H., Shlosman I., de Jong R. S., 1995a, ApJ, 454, 623
Knapen J. H., Beckman J. E., Shlosman I., Peletier R. F., Heller C. H., de Jong R. S., 1995b, ApJ, 443, L73
Kormendy J., 1981, in Fall S. M., Lynden-Bell D., eds, Structure and Evolution of Normal Galaxies. Cambridge Univ. Press, Cambridge, p. 85
Kormendy J., 1982, ApJ, 257, 75
Kormendy J., 1983, ApJ, 275, 529
Kormendy J., 1984, ApJ, 286, 209
Kormendy J., Kennicutt R. C. Jr, 2004, ARA&A, 42, 603 (KK2004)
Kormendy J., Cornell M. E., Block D., Knapen J. H., Allard E. L., 2006, ApJ, 642, 765
Kuijken K., Merrifield M. R., 1995, ApJ, 443, L13
Laurikainen E., Salo H., 2002, MNRAS, 337, 1118
Laurikainen E., Salo H., Rautiainen P., 2002, MNRAS, 337, 880
Laurikainen E., Salo H., Buta R., 2004a, ApJ, 607, 103
Laurikainen E., Salo H., Buta R., Vasylyev S., 2004b, MNRAS, 355, 1251
Laurikainen E., Salo H., Buta R., 2005, MNRAS, 362, 1319
Laurikainen E., Salo H., Buta R., Knapen J., Speltincx T., Block D., 2006a, AJ, 132, 2634
Laurikainen E., Salo H., Buta R., 2006b, in Combes F., Palous J., eds, IAU Symp. 235, Galaxy Evolution Across the Hubble Time. Prague, p. 9
Lima-Neto G. B., Combes F., 1995, A&A, 294, 657
Lüticke R., Dettmar R. J., Pohlen M., 2000, A&AS, 145, 435
Lynden-Bell D., Kalnajs A. J., 1972, MNRAS, 157, 1
Magrelli G., Bettoni D., Galletta G., 1992, MNRAS, 256, 500
Marinova I., Jogee S., 2006, MNRAS, 346, 251
Martin P., 1995, AJ, 109, 2428
Martinez-Valpuesta I., Shlosman I., 2004, ApJ, 613, L29
Martinez-Valpuesta I., Shlosman I., Heller C., 2006, ApJ, 637, 214
McElroy D. B., 2004, ApJS, 100, 105
Merrifield M. R., Kuijken K., 1995, MNRAS, 274, 933
Moiseev A. V., Valdës J. R., Chavushyan V. H., 2004, A&A, 421, 433
Ohta K., 1996, in Buta R., Crocker D. S., Elmegreen B. G., eds, IAU Coll. 157, Barred Galaxies. p. 37
Ohta K., Hamabe M., Wakamatsu K., 1990, ApJ, 357, 71
O'Neil J. K., Dubinski J., 2003, MNRAS, 251
Palacios J., Garcia-Vargas M. L., Diaz A., Terlevich R., Terlevich E., 1997, A&A, 323, 749

Persic M., Salucci P., Stel F., 1996, MNRAS, 281, 27
Pfenniger D., Friedli D., 1991, A&A, 252, 75
Pizzella A., Corsini E. M., Vega Belträn J. C., Bertola F., 2004, A&A, 424, 447
Raha N., Sellwood J. A., James R. A., Kahn F. D., 1991, Nat, 352, 411
Rand R. J., Wallin J. F., 2004, ApJ, 614, 412
Rautiainen P., Salo H., Laurikainen E., 2005, ApJ, 631, L129
Regan M. W., Elmegreen D. M., 1997, AJ, 114, 965
Romanowsky A. J., 2004, preprint (astro-ph/0411797)
Romanowsky A. J., 2006, in Barlow M. J., Mendez R. H., eds, IAU Symp. 234, Planetary Nebulae in Our Galaxy and Beyond. Cambridge Univ. Press, Cambridge
Sakamoto K., Okumura S. K., Ishizuki S., Scoville N. Z., 1999, ApJ, 525, 691
Salo H., Rautiainen P., Buta R., Purcell G., Cobb M., Crocker D. A., Laurikainen E., 1999, AJ, 117, 792
Salo H., Laurikainen E., Rautiainen P., Buta R., 2006, in Combes F., Palous J., eds, IAU Symp. 235, Galaxy Evolution Across the Hubble Time. Prague, p. 347
Searle L., Zinn R., 1978, ApJ, 225, 357
Schechter P. L., Dressler A., 1987, AJ, 94, 563
Schultz J., Fricke U., Alvensleben V., Fricke K. J., 2003, A&A, 389, 89
Schweizer F., 2005, in de Grijs R. M., Gonzalez Delgado, eds, Starbursts: From 30 Doradus to Lyman Break Galaxies. Springer-Verlag, Dordrecht, p. 143
Sellwood J. A., 1980, A&A, 89, 296
Shapiro K. L., Gerssen J., van der Marel R. P., 2003, AJ, 126, 2707
Sheth K., Vogel S. N., Regan M. W., Thornley M. D., Teuben P. J., 2005, ApJ, 632, 217
Shlosman I., Peletier R. F., Knapen J. H., 2000, ApJ, 535, L83
Simien F., de Vaucouleurs G., 1986, ApJ, 302, 564
Simien F., Prugniel Ph., 1997, A&AS, 126, 15
Springel V., Hernquist L., 2005, ApJ, 622, L9
Steffen A. T., Barger A. J., Cowie L. L., Mushotsky R. F., Yaung Y., 2003, ApJ, 596, L23
Steinmetz M., Navarro J. F., 2002, New Astron., 7, 155
Toomre A., Toomre J., 1972, ApJ, 178, 623
Tremaine S., 1989, in Sellwood J. A., ed., Dynamics of Astrophysical Discs. Cambridge Univ. Press, Cambridge, p. 231
Ueda Y., Masayuki A., Ohta K., Miyaji T., 2003, ApJ, 598, 886
White S. D. M., Rees M. J., 1978, MNRAS, 183, 341
Whyte L., Abraham R. G., Merrifield M. R., Eskridge P. B., Frogel J. A., Pogge R. W., 2002, MNRAS, 336, 1281
Zhang X., 1998, ApJ, 499, 93
Zhang X., Buta R., 2007, AJ, 133, 2584

This paper has been typeset from a TEX/LATEX file prepared by the author.